

**“Evaluation and Characterization of In-Line Annealed Continuous Cast Aluminum  
Sheet ”  
Annual Project Report  
(DE-FC07-01ID14024)**

**Prepared by**

**Secat, Inc.  
January 2002**

**SECAT, Inc.  
Coldstream Research Campus  
1505 Bull Lea Road  
Lexington, Kentucky 40511  
Telephone 859-514-4989  
Fax 859-514-4988  
E- mail : [skdas@engr.uky.edu](mailto:skdas@engr.uky.edu)**

## **1. Introduction**

The goal of this project is to develop optimized, energy-efficient thermo-mechanical processing procedures for in-line annealing of continuously cast hot bands of two 5000 series aluminum alloys (5754 and 5052). The implementation of the R&D will result in the production of sheet with improved formability at high levels of productivity, consistency, and quality.

The proposed R&D involves the following efforts:

- Design and build continuous in-line annealing equipment for plant-scale trials
- Carry out plant-scale trials at Commonwealth Aluminum Corp.'s (CAC) plant in Carson, CA
- Determine the effects of processing variables on the microstructure, texture, mechanical properties, and formability of aluminum sheet
- Optimize the processing variables utilizing a metallurgical model for the kinetics of microstructure and texture evolution during thermo-mechanical processing
- Develop design parameters for commercial implementation
- Conduct techno-economic studies of the recommended process equipment to identify impacts on production costs

## **2. Project Kickoff Meeting:**

A kickoff meeting on the above project was held in Lexington, KY, on November 10, 2000. Dr. Zhong Li of Commonwealth Aluminum summarized the overall scope and goal of the project. Team members from Oak Ridge National Laboratory (Dr. Ian Anderson, Dr. Craig Blue, Dr. Kenneth Liu and Dr. B. Radhakrishnan) made brief presentations on the unique facilities available at Oak Ridge for the project. Rapid heating using IR lamps, high temperature compression testing at high strain rates, Orientation Imaging Microscopy (OIM) techniques for determination of texture and the computational tools available to model the evolution of microstructure during deformation and annealing were discussed. Representatives from Ajax discussed the induction-heating unit needed to meet the requirements for the project. Dr. Amit Ghosh of the University of Michigan discussed formability testing methods and some formability data from 6xxx series aluminum alloys. Dr. Morris from the University of Kentucky discussed some earlier work carried out on annealing of continuously cast aluminum alloys.

## **3. Plant Visit and Project Review Meeting:**

Project personnel visited the Uhrichsville plant of Commonwealth Aluminum in Ohio on January 26<sup>th</sup> and held a review meeting. Dr. Zhong Li of Commonwealth Aluminum provided information on line speeds, gauge thickness, and hot reduction schedules for the two alloys of interest. He also provided a list of suggested baseline experimental work that needs to be done on alloys 5052 and 5754. After some discussion about the scope of these tasks and in view of the limited funds available for characterization at Oak Ridge, it was agreed that most of this work would be conducted at the Universities of Kentucky and Michigan. Dr. Huxford made a brief presentation on the Plasma Arc IR heating

facility at Oak Ridge and the power densities that can be achieved at various lamp lengths. Mr. Valenti of Ajax indicated the their induction system can heat strip from 500°F to 900°F in about 0.75 sec. There was considerable discussion on various methods that could be used to produce rapidly heated samples for some baseline studies. A “Gleeble” testing unit and the Plasma Arc IR facility at Oak Ridge as well as an induction strip-heating unit at Ajax were considered. Of all these, the “Gleeble” was considered to be the quickest way to get rapidly heated samples.

Based on the discussions at the initial kick-off meeting at Secat and the review meeting at Uhrichsville, the following tasks were set for the project participants.

- University of Kentucky: Determination of texture and mechanical properties of continuously cast AA5754 Al Alloy as a function of cold rolling and annealing parameters
- University of Michigan: Determine the formability of continuously cast AA5052 alloys as a function of cold rolling and annealing parameters.
- Oak Ridge National Laboratory: (1) Advanced characterization of the AA5052 and AA5754 hot bands using EBSD technique to determine the microtexture and its variation through the thickness of the sheet (2) Determine the high temperature mechanical properties of AA5754 hot band to provide input for modeling the deformation behavior of the alloy during hot rolling (3) Develop techniques for providing laboratory samples of rapidly annealed hot band for formability studies (4) Model the microstructure evolution during in-line recrystallization of hot band.
- Ajax and Commonwealth: (1) Design, fabricate and install in-line induction heating facility at the Carson, California plant and evaluate its performance (2) Conduct plant trials of in-line annealing.

#### **4. Technical Progress**

The following sections provide a detailed description of the technical progress made by the project participants during first year of the project.

##### **4.1 University of Kentucky: Texture and Mechanical Properties of Strip Cast AA5754 Al Alloy**

###### **Background**

This report contains the findings of a comprehensive study of the microstructure, texture and mechanical properties of strip cast AA5754 alloys utilizing different hot band gauges and thermomechanical processing routes.

## **Materials and Experimental**

The materials used in the study are hot bands of AA5754 alloy with three different hot band gauges (0.080", 0.120" and 0.160" gauges). They were produced by Commonwealth Aluminum Company using the Hazelett strip cast process, and all are in a hot rolled condition.

### Six processing routes

The 0.080" hot bands (i.e. #1 treatment) were annealed at 700, 750, 800, 850, and 950 °F in a salt bath (soaking time 10mins) and in a normal furnace (soaking time 3hrs, heat-up rate 1.7 °F/min), respectively.

The 0.120" hot bands were cold rolled to 0.080" (i.e. #2 treatment), then annealed at 700, 750, 800, 850, and 950 °F in a salt bath (soaking time 10mins) and in a normal furnace (soaking time 3hrs, heat-up rate 1.7 °F/min), respectively.

The 0.160" hot bands were cold rolled to 0.080" (i.e. #3 treatment), then annealed at 700, 750, 800, 850, and 950 °F in a salt bath (soaking time 15mins) and in a normal furnace (soaking time 3hrs, heat-up rate 1.7 °F/min), respectively.

The 0.160" hot bands were homogenized at 900 °F (3hrs) in a normal furnace (i.e. #4 treatment), then cold rolled to 0.080" and annealed at 700, 750, 800, 850, and 950 °F in a salt bath (soaking time 10mins) and in a normal furnace (soaking time 3hrs, heat-up rate 1.7 °F/min), respectively.

0.160" hot bands were homogenized at 900 °F (3hrs) in a salt bath (i.e. #5 treatment), then cold rolled to 0.080" and annealed at different temperatures from 500 °F to 950 °F in a salt bath (soaking time 10mins) and in a normal furnace (soaking time 3hrs, heat-up rate 1.7 °F/min), respectively.

The 0.160" hot bands were homogenized at 900 °F (0.5 hr) in a salt bath (i.e. #6 treatment), then cold rolled to 0.080" and annealed at different temperatures from 500 °F to 950 °F in a salt bath (soaking time 10mins) and in a normal furnace (soaking time 3hrs, heat-up rate 1.7 °F/min), respectively.

#1, #2, #3, #4, #5 and #6 will be used to refer to the above treatments respectively in the later sections of this report.

### Tensile test, earing test and Olsen test

The tensile properties (ultimate tensile strength- UTS, yield strength- YS and elongation rate- EL) of samples from the above cold rolling and annealing conditions were measured and were shown in Fig.1-23. Three samples were tested for each condition. Earing tests and Olsen tests (two samples for each condition) were run and were conducted at Commonwealth Aluminum in Lewisport, Kentucky.

### Texture measurement

Texture analyses of samples in the required conditions (i.e. cold rolling and annealing at 700 °F and 950 °F in a salt bath and in a normal furnace) were determined in the surface region of the sample (see Table 1-3). (111), (200), and (220) pole figures were measured up to a maximum tilt angle of 70° by the Schulz back-reflection method using  $\text{CuK}\alpha$  radiation. The ODFs were calculated from three incomplete pole figures using the series expansion method with expansion to  $l_{\text{max}} = 16$ .

## Microstructures

The microstructures (grain and particle structures) of the samples in the above cold rolling and annealing conditions were examined on the longitudinal section of the samples. They were all electro-polished and finally anodized before optical microscopic examination.

## **Summary**

1. There is a small increase in tensile strength (less than 1 ksi) after cold rolling (from 0.120" to 0.080" and 0.160" to 0.080") and annealing, in comparison to those of the directly annealed 0.080" hot band. This suggests that a greater degree of cold work before annealing will produce a small but progressive increase in tensile properties (less than 1 ksi) after annealing.
2. The 0.080" hot band in an annealed condition yields 0° and 90° earing in both salt bath and normal furnace conditions. Earing (%) increases slightly with increase in anneal temperature (700 °F to 950 °F). There is only a small (not important) difference in earing between furnace anneal and salt bath anneal.
3. For the 0.120" hot band cold rolled to 0.080" the earing is 45°. 45° earing decreases slightly as the anneal temperature is increased from 700 °F to 950 °F (1.53, 1.21 to 0.77, 0.66). There is little difference in earing for furnace anneal vs. salt bath anneal.
4. For 0.160" hot band cold rolled to 0.080" there is a small reduction in 45° earing as the anneal temperature is increased from 700 °F to 950 °F. There is little effect on earing using a furnace anneal vs. a salt bath anneal.
5. For 0.160" hot band, homogenized at 900 °F and then cold rolled to 0.080" the earing values are higher than for #1, #2, #3 treatments when furnace annealing is employed.
6. All earing results are 45° for the 0.160" hot bands homogenized at 900 °F for 3 hours and 0.5 hour in a salt bath with the earing decreasing as the anneal temperature is increased. Furnace annealing yields slightly higher earing than does salt bath annealing.
7. In general, the Olsen values at 700 °F for all #1-#6 treatments are comparable to those at 900 °F. There is little effect of furnace anneal vs. salt bath. Specifically,
  - 1) For #1 and #2 treatments the Olsen values are slightly higher at 700 °F anneal than at 950 °F anneal. No effect is seen in furnace anneal vs. salt bath anneal.
  - 2) For #4 treatment the Olsen values are higher than for #1, #2, #3 treatments and range from 0.375" to 0.398".
  - 3) For treatment of the 0.160" hot bands at 900 °F for 3 hours (#5 treatment) and 0.5 hour (#6 treatment) in a salt bath all Olsen values are similar and range from 0.375" to 0.390".
8. After annealing the volume fraction of the cube component is higher for #1 treatment vs. #2 treatment and the  $\delta$  values for treatment #1 are lower than for #2 treatment.
9. After annealing for #1 and #2 treatments, the random component is greater than 60% (range 60.5% to 67.2%).
10. After annealing, the random component for #3 and #4 treatments is greater than for #1 and #2 treatments.

11. The  $\delta^*$  values for #3 and #4 treatments are in the range 12.1-21.3), compared with a range of 11.1-18.9 for #1 and #2 treatments.
12. Random component values for 0.160" hot bands homogenized at 900 °F for 3 hours and 0.5 hour in a salt bath are intermediate between those for #1 and #2 treatments or those for #3 and #4 treatments. They range from 64.7% to 71.8%.
13. The  $\delta^*$  values for the 0.160" hot bands homogenized at 900 °F for 3 hours and 0.5 hour in a salt bath (range 14.5-25.8) tend to be higher than the  $\delta$  values for either #1 and #2 treatments or #3 and #4 treatments. This correlates with the general observation that the earing is higher for the 0.160" hot bands homogenized at 900 °F for 3 hours and 0.5 hour in a salt bath when compared to #1, #2 or #3 treatment.
14. In general, it appears that there is not a great difference in properties, i.e., mechanical tensile properties, earing values, and Olsen values when the 6 treatments are compared with each other. Only minor differences, previously pointed out, exist. Therefore it would appear that treatment #1 could be considered most desirable in order to produce 0.080" gauge AA 5754 alloy since it is the simplest and thus the most economical of the thermomechanical processes evaluated.  
However it could be expected that variation in properties (across the coil width as well as along the length of the coil) would be greater in treatment #1 than in the more complex treatments, #2-#6.  
This greater variation in properties in treatment #1 could be expected due to greater variation in total structure than in the more complex treatments. The general rule with regard to variation in structure is—the more processing of the hot band that is carried out the less is the variation in structure. Hot bands themselves can possess significant variation in solute supersaturation across the width of a coil as well as a variation in particle structure. Thus, in the final analysis, the degree of variation in properties may be the overriding determining factor in selecting a particular thermomechanical process to employ in order to produce CC, AA5754 aluminum alloy for automotive body application.

---

\* The  $\delta$  value is defined as  $\Sigma(\text{Cu+B+S+Rcube})-\Sigma(\text{Cube+G})$ .

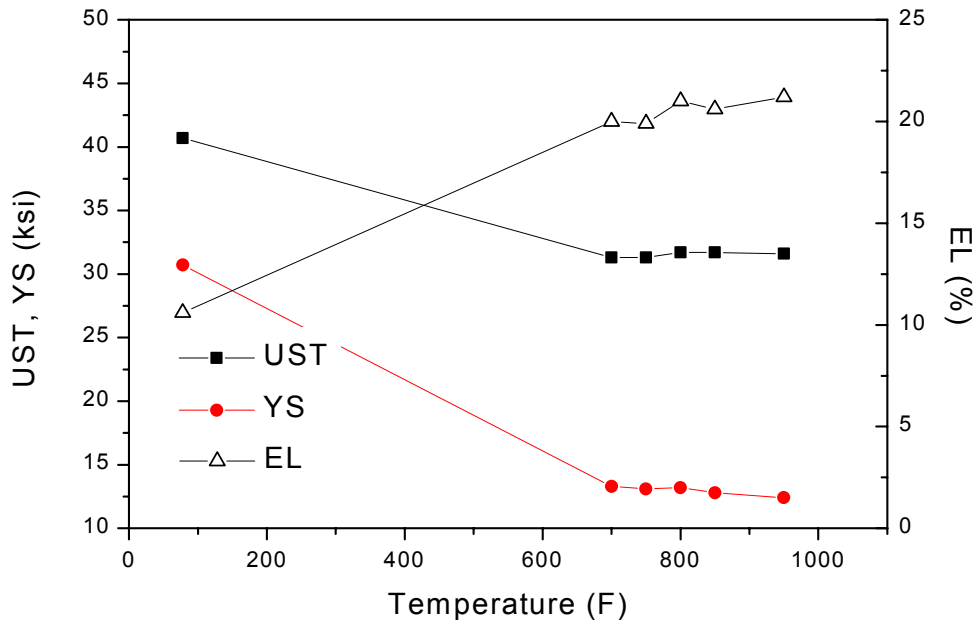


Fig. 1 The tensile properties of the 0.08" hot bands annealed at different temperatures (3 hrs) AA5754 Alloy

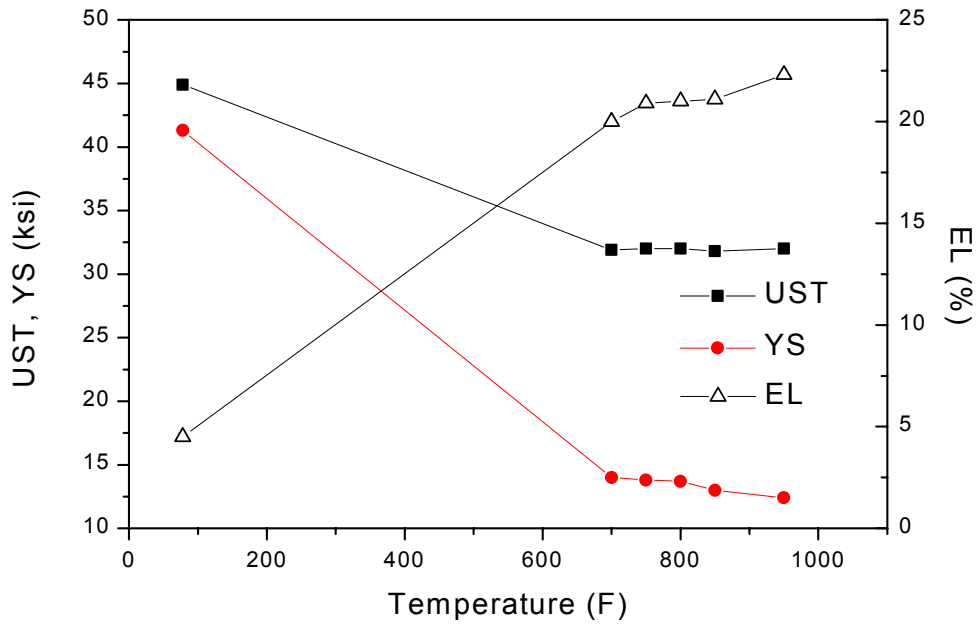


Fig. 2 The tensile properties of the 0.120" hot bands cold rolled to 0.08", then annealed at different temperatures (3 hrs) AA5754 Alloy

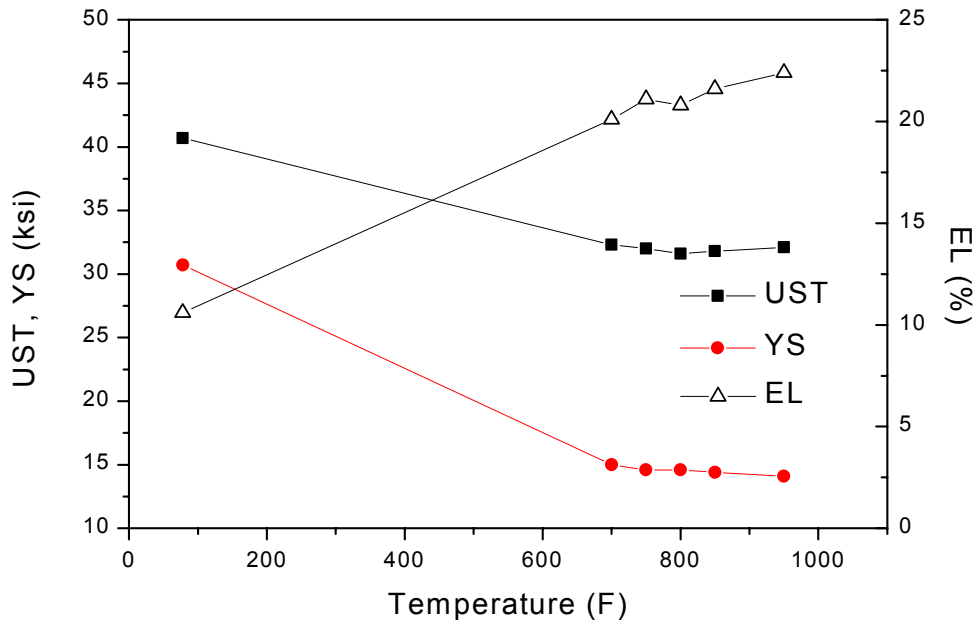


Fig. 3 The tensile properties of the 0.08" hot bands annealed in salt bath at different temperatures (10 mins) AA5754 Alloy

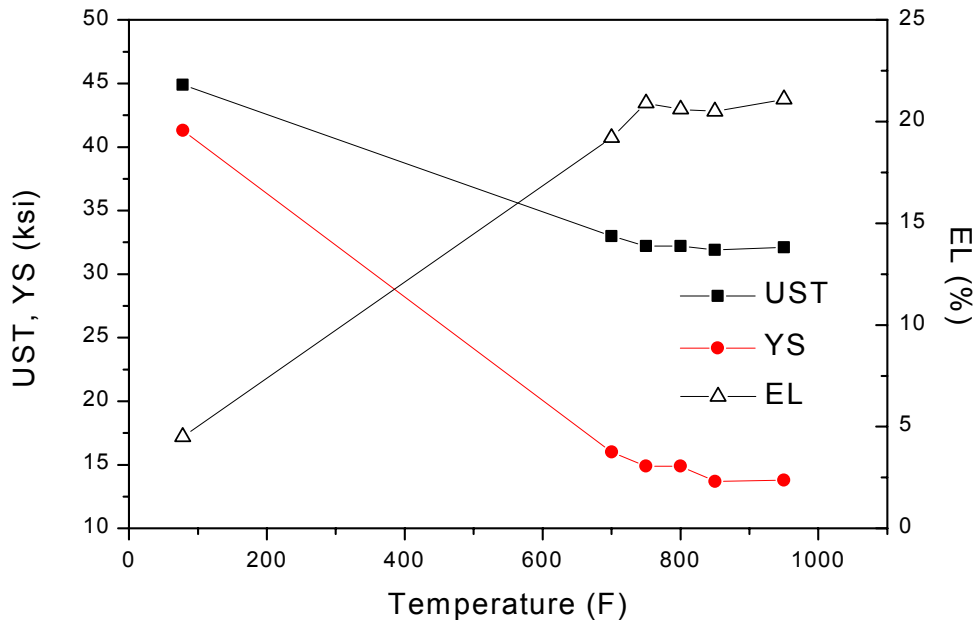


Fig. 4 The tensile properties of the 0.120" hot bands cold rolled to 0.08", then annealed in salt bath at different temperatures (10 mins) AA5754 Alloy

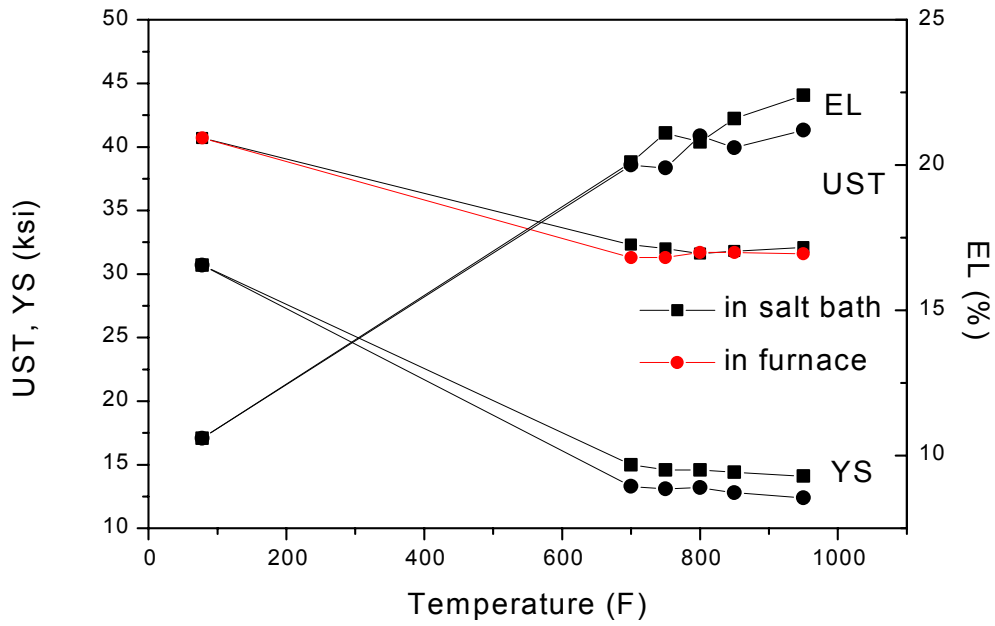


Fig. 5 Comparing tensile properties of the 0.080" hot band after annealing in salt bath and in a normal furnace

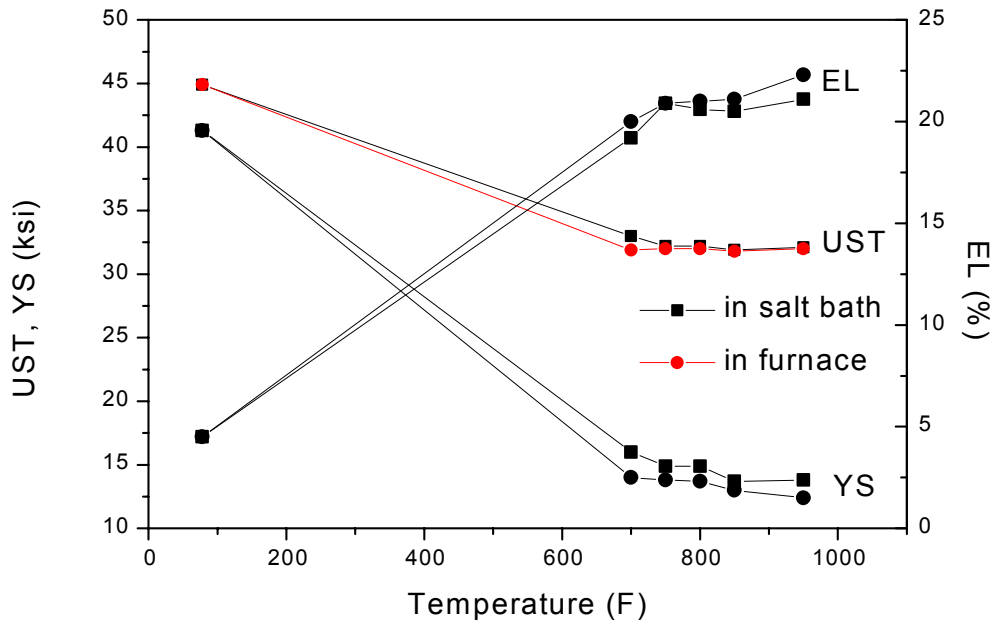


Fig. 6 Comparing tensile properties of the 0.120" hot band cold rolled to 0.080" then annealed in a salt bath and in a normal furnace

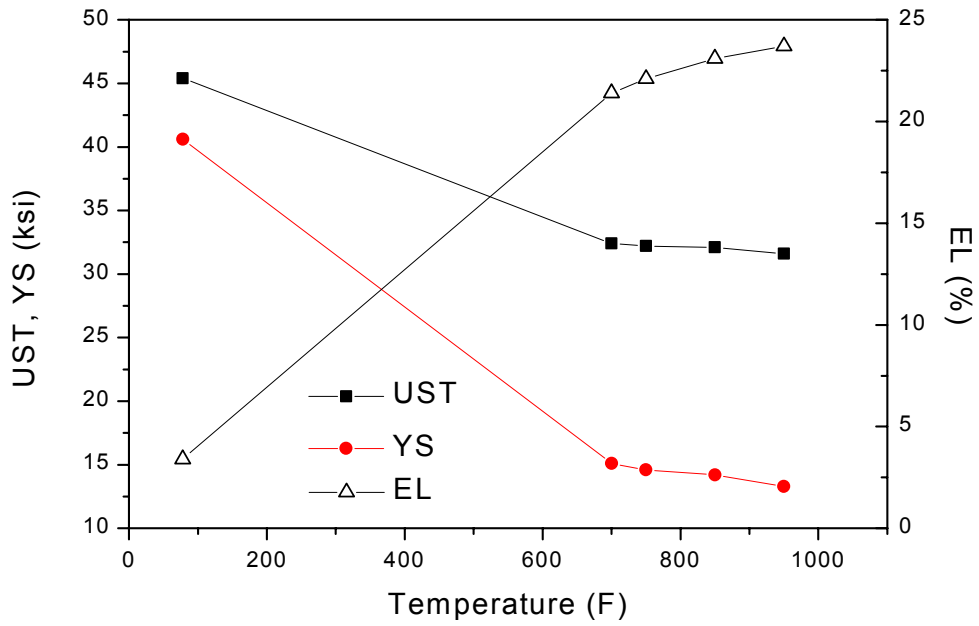


Fig. 7 The tensile properties of the 0.160” hot bands cold rolled to 0.080”, then annealed in a slat bath at different temperatures (10 mins) AA5754 alloy

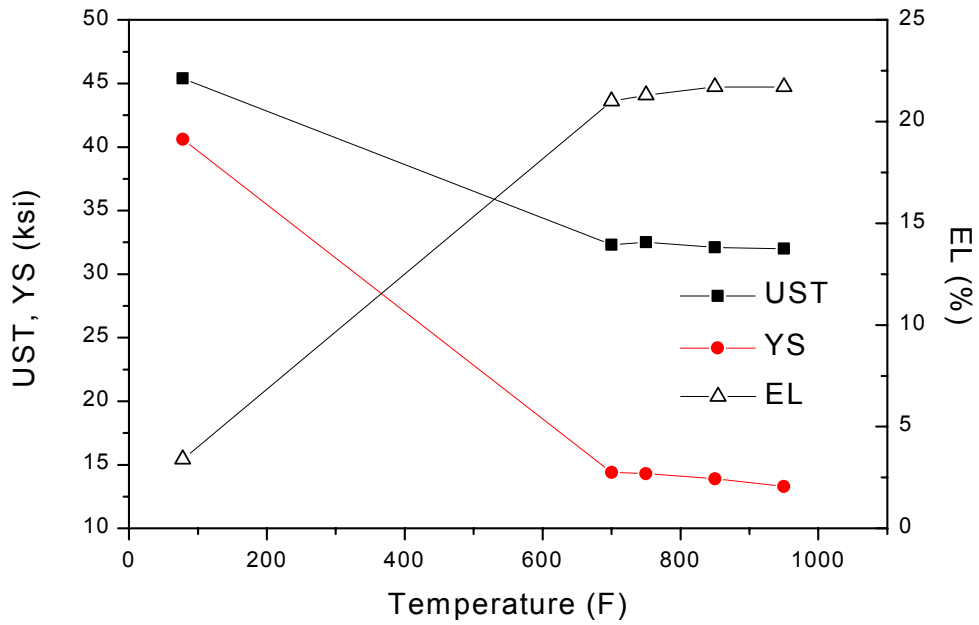


Fig. 8 The tensile properties of the 0.160” hot bands cold rolled to 0.080”, then annealed at different temperatures (3 hrs) AA5754 alloy

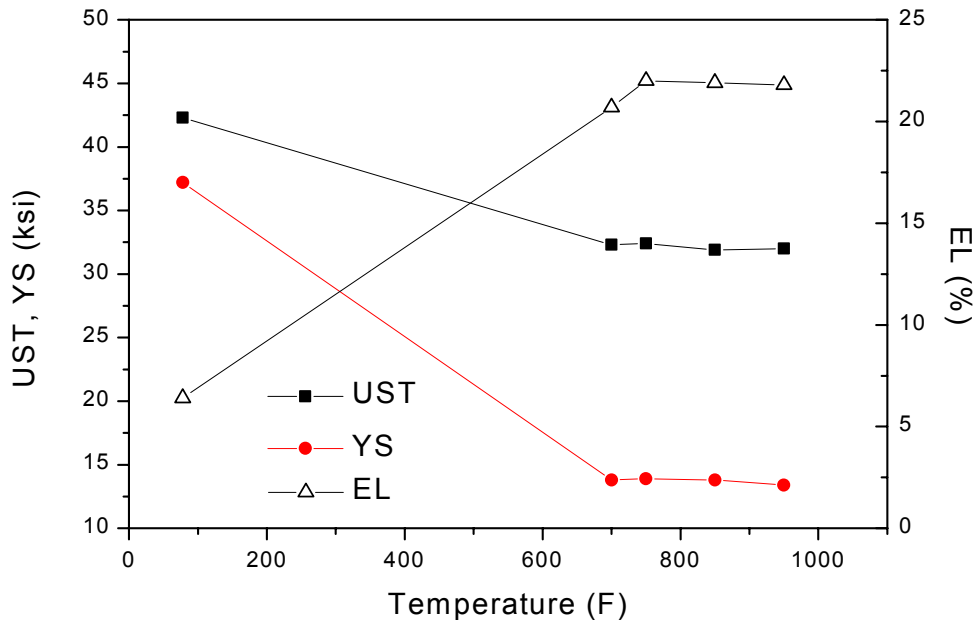


Fig. 9 The tensile properties of the 0.160" hot band plus 900 °F homogenization then cold rolled to 0.080" and annealed in slat bath at different temperatures (10 mins) AA5754 alloy

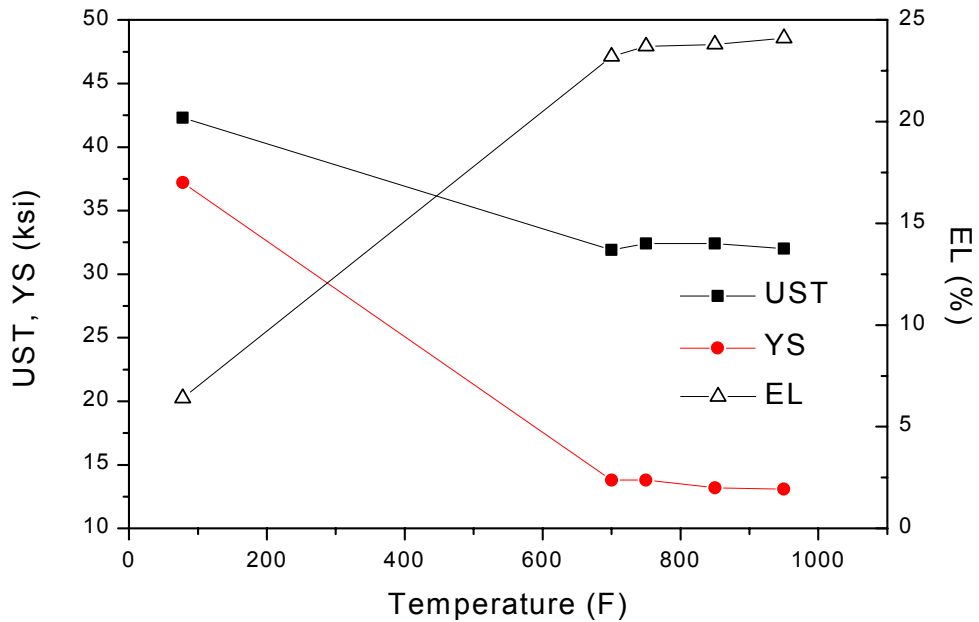


Fig. 10 The tensile properties of the 0.160" hot band plus 900 °F homogenization then cold rolled to 0.080" and annealed at different temperatures (3 hrs) AA5754 alloy

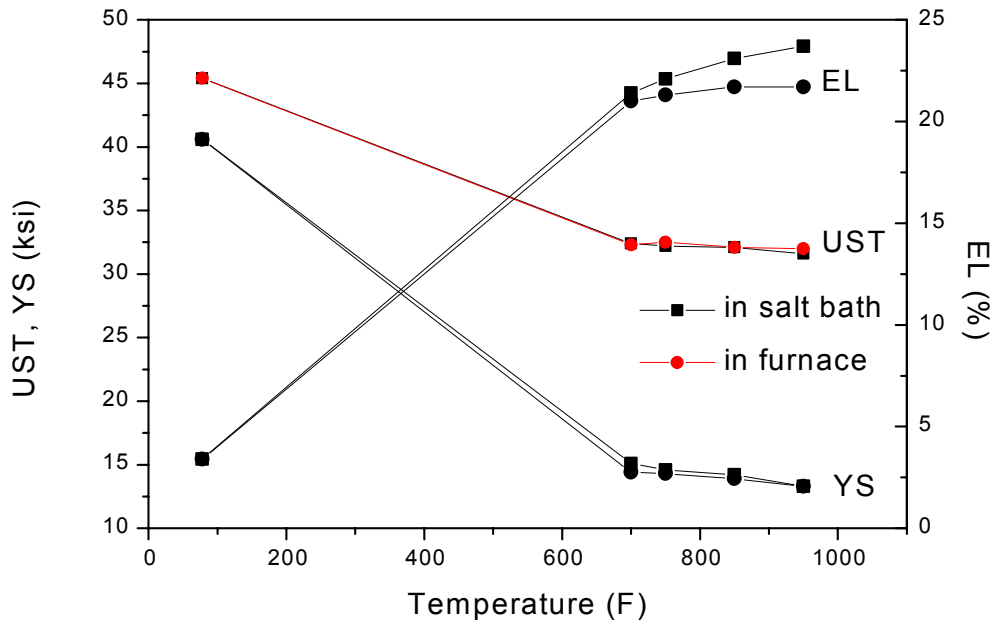


Fig. 11 Comparing tensile properties of the 0.120" hot band cold rolled to 0.080" then annealed in a salt bath and in a normal furnace

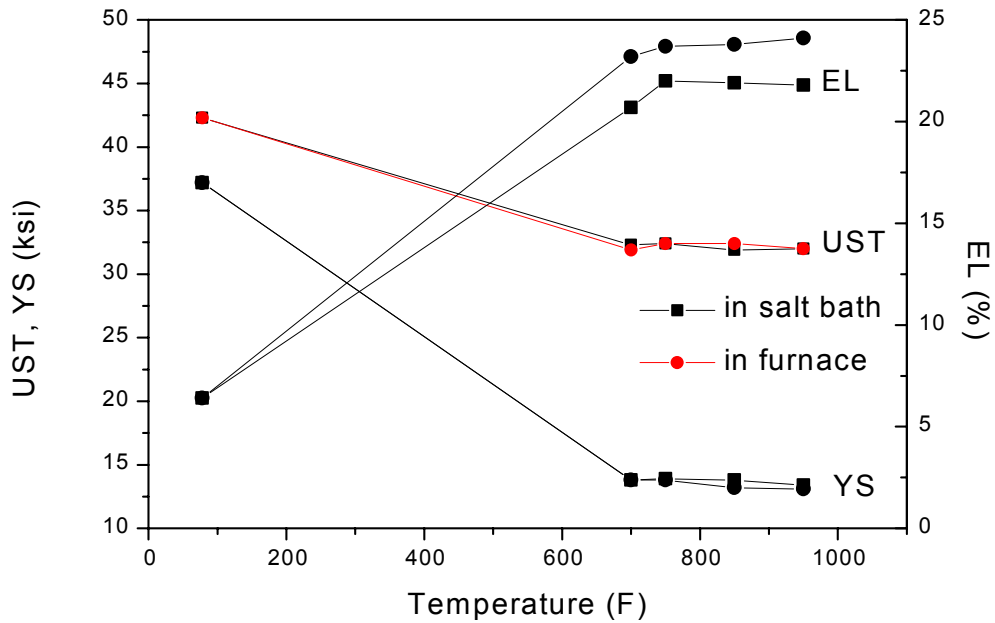


Fig. 12 Comparing tensile properties of the 0.160" hot band plus 900 °F homogenization then cold rolled to 0.080" and annealed at different temperatures in a salt bath and in a normal furnace

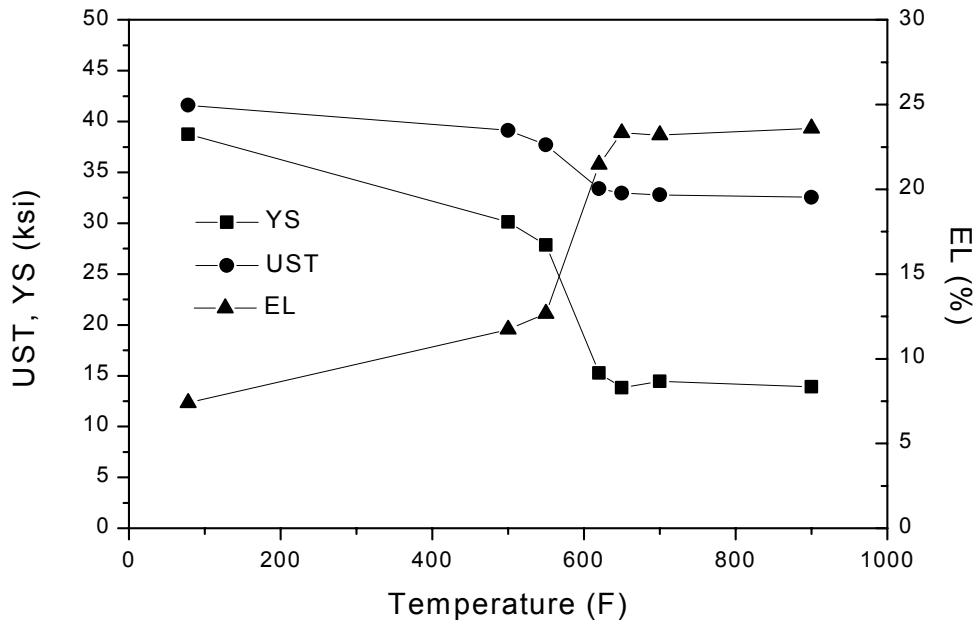


Fig. 13 The tensile properties of the 0.160" hot band homogenized at 900 °F (3 hrs) in a salt bath, then cold rolled to 0.080" and annealed at different temperature in a salt bath

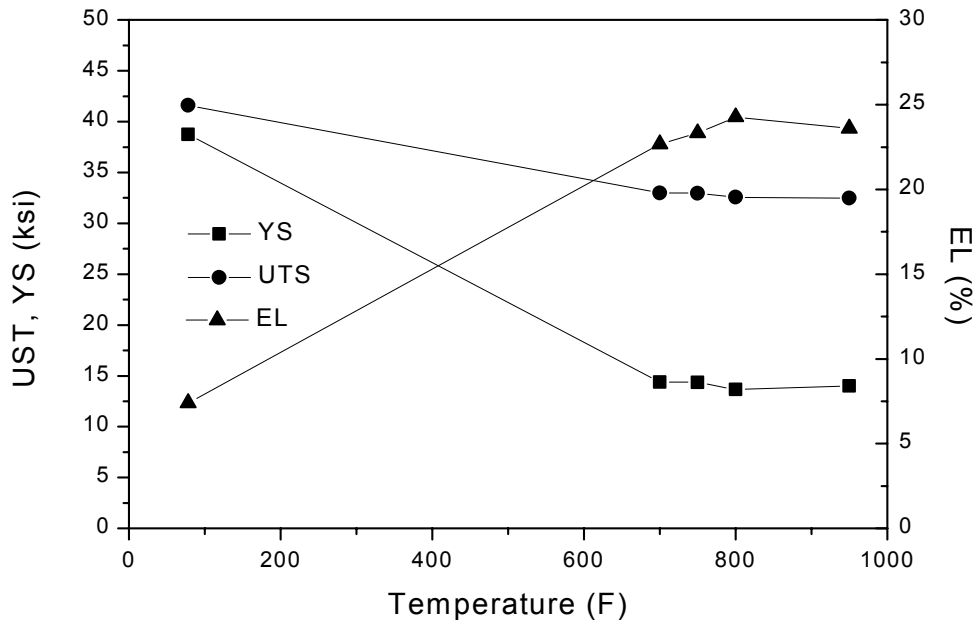


Fig. 14 The tensile properties of the 0.160" hot band homogenized at 900 °F (3 hrs) in a salt bath, then cold rolled to 0.080" and annealed at different temperature in a normal furnace

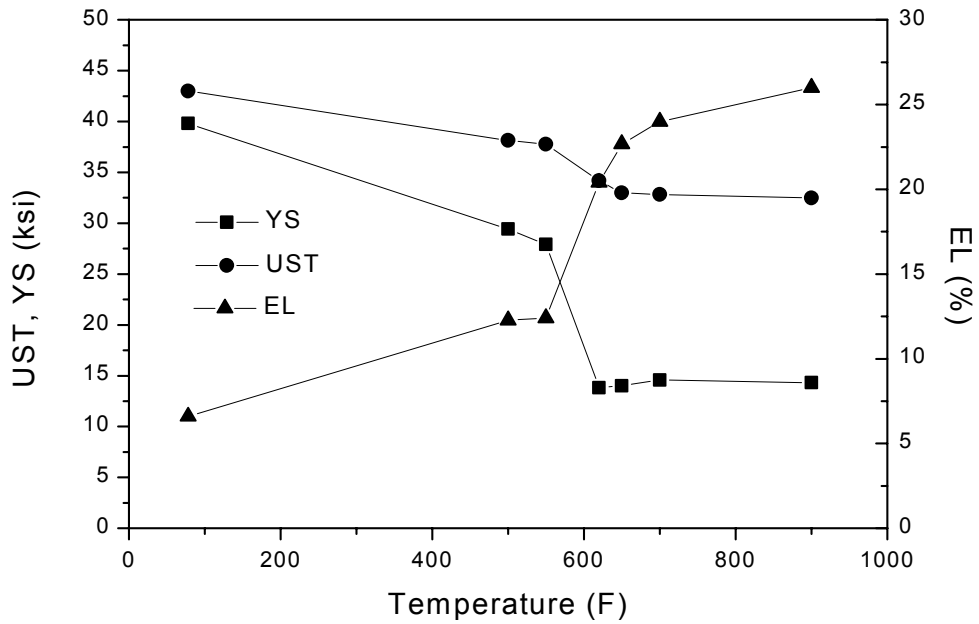


Fig. 15 The tensile properties of the 0.160" hot band homogenized at 900 °F (0.5 hrs) in a salt bath, then cold rolled to 0.080" and annealed at different temperature in a salt bath

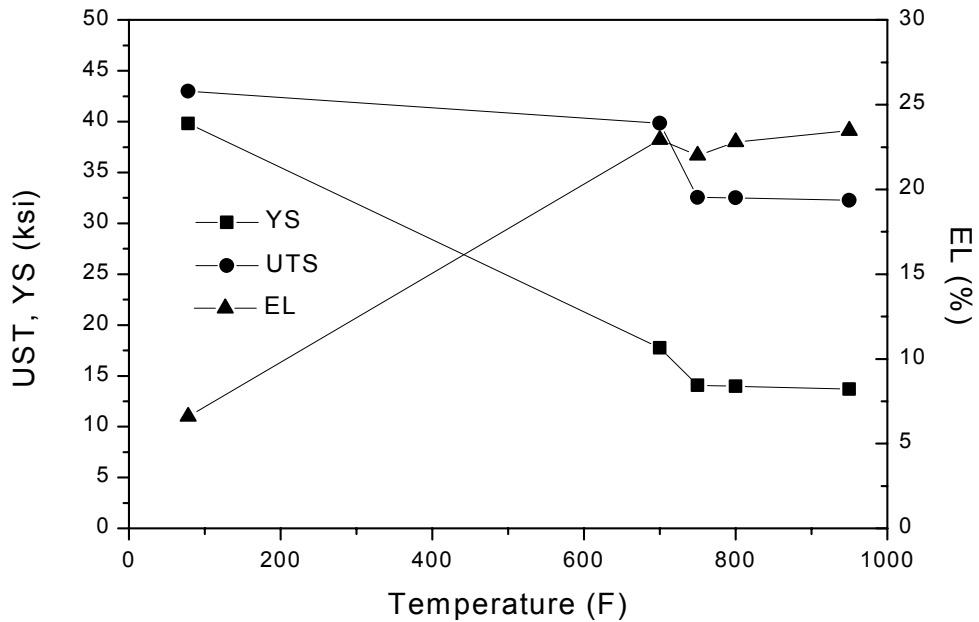


Fig. 16 The tensile properties of the 0.160" hot band homogenized at 900 °F (0.5 hrs) in salt bath, then cold rolled to 0.080" and annealed at different temperature in a normal furnace

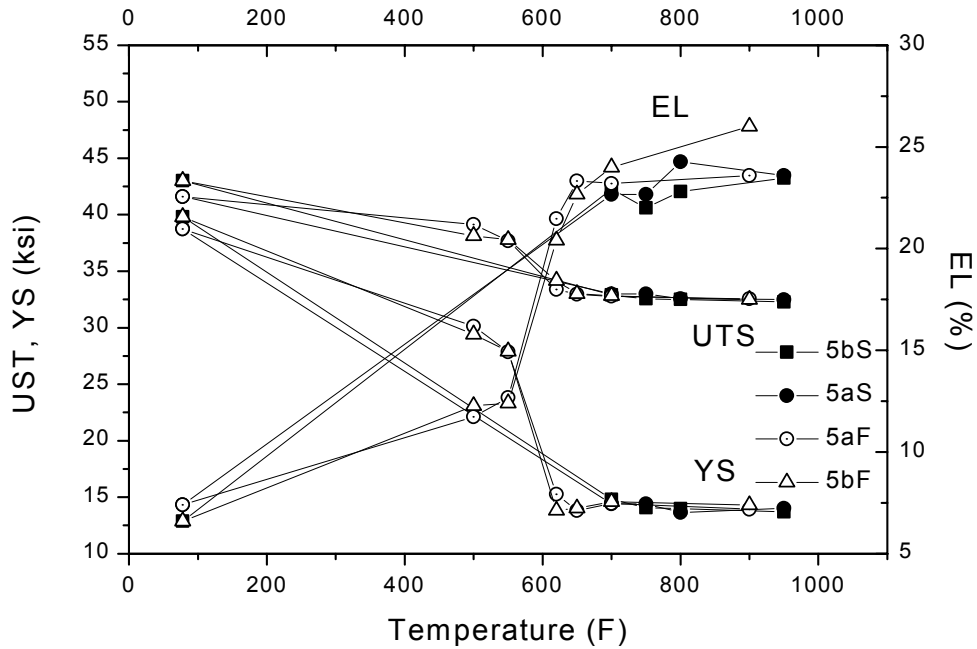


Fig. 17 Comparison of tensile properties between 5aS, 5bS, 5aF and 5bF samples.  
**5aS** represents the 0.160" hot band, preheat treated at 900 °F (3 hrs) in a salt bath, cold rolled to 0.080" and then annealed at different temperatures in a normal furnace;  
**5bS** is the 0.160" hot band preheat treated at 900 °F (0.5 hr) in a salt bath, cold rolled to 0.080" and then annealed at different temperatures in a normal furnace;  
**5aF** The 0.160" hot band preheat treated at 900 °F (3 hrs) in a salt bath, cold rolled to 0.080" and then annealed at different temperatures in a salt bath;  
**5bF** The 0.160" hot band preheat treated at 900 °F (0.5 hr) in a salt bath, cold rolled to 0.080" and then annealed at different temperatures in a salt bath.

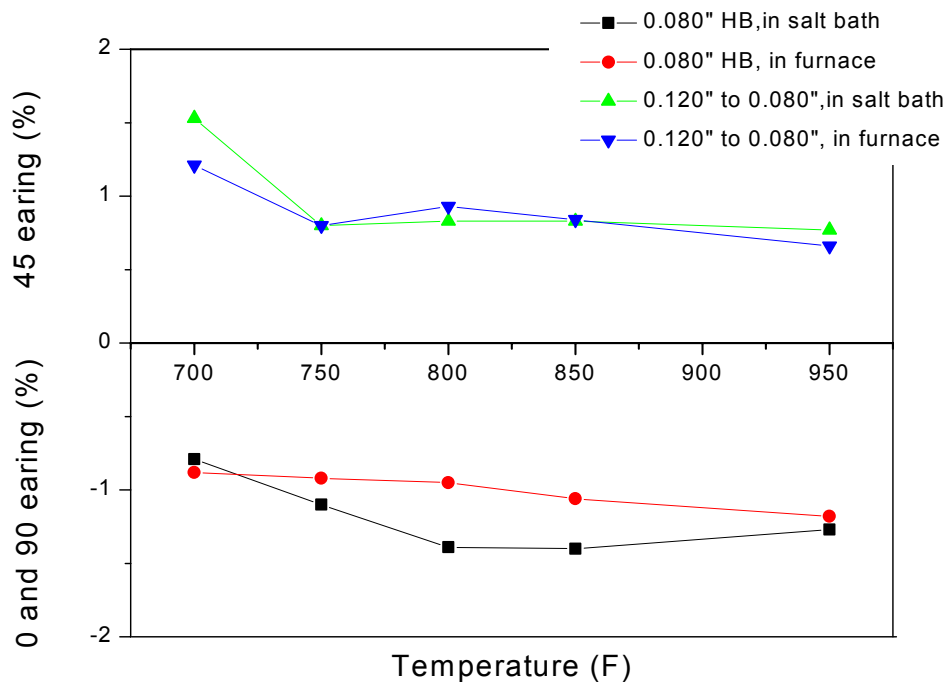


Fig. 18 Earing (%) Of the 0.080" hot band and the 0.120" hot band cold rolled to 0.080", then annealed at different temperatures

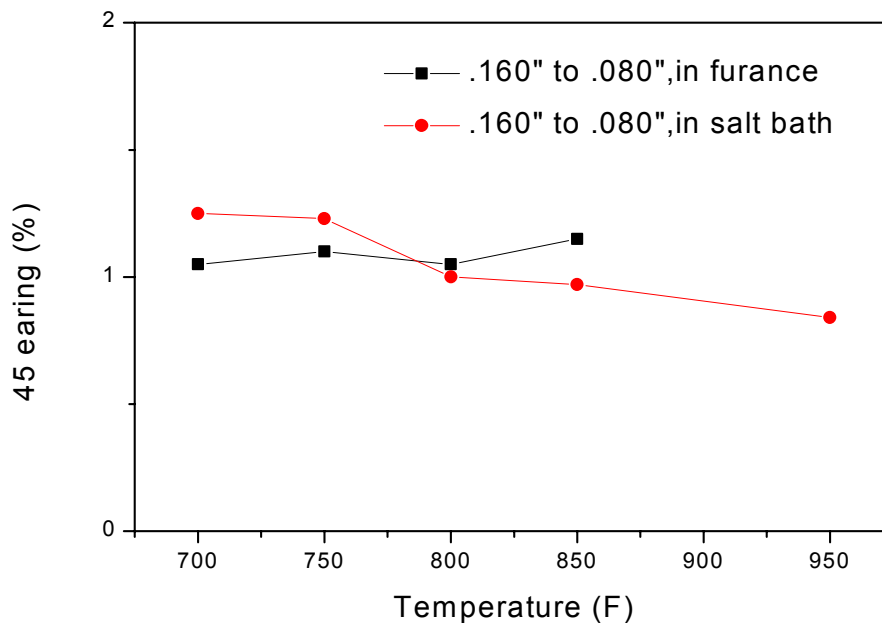


Fig. 19 Earing (%) of the 0.160" hot band cold rolled to 0.080", then annealed at different temperatures in a salt bath and in a normal

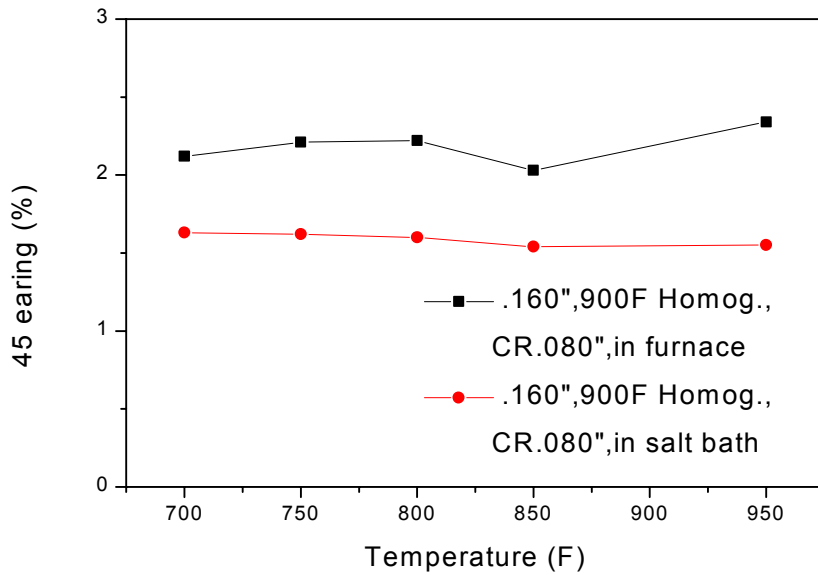


Fig. 20 45° Earing (%) of the 0.160” hot band homogenized at 900 °F (3 hrs) in a furnace, then cold rolled to 0.080” and annealed at different temperatures in a salt bath and in a furnace

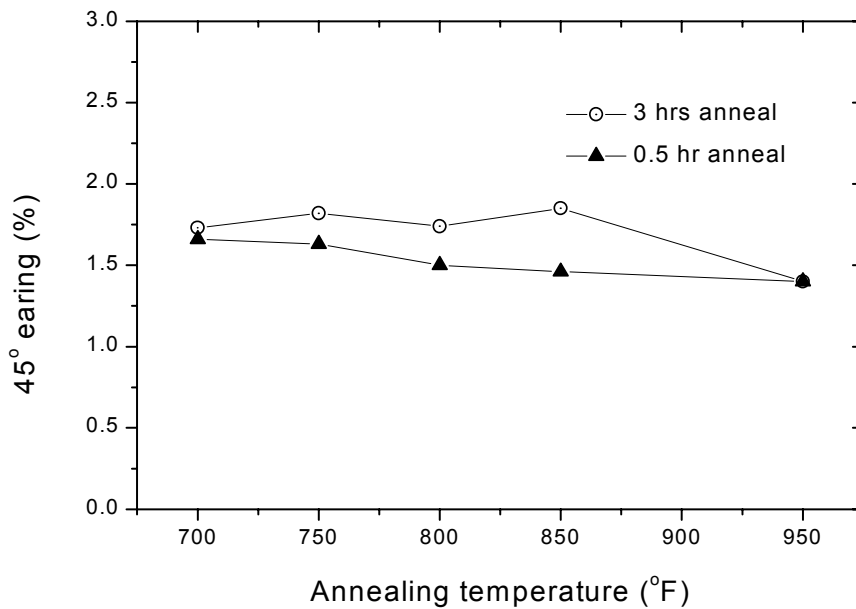


Fig. 21 Earing values after the 0.160” hot band homogenized at 900 F in a salt bath for 3 hours and 0.5 hour respectively, cold rolled to 0.080” and annealed at a normal heat-up rate (1.7 °F/min).

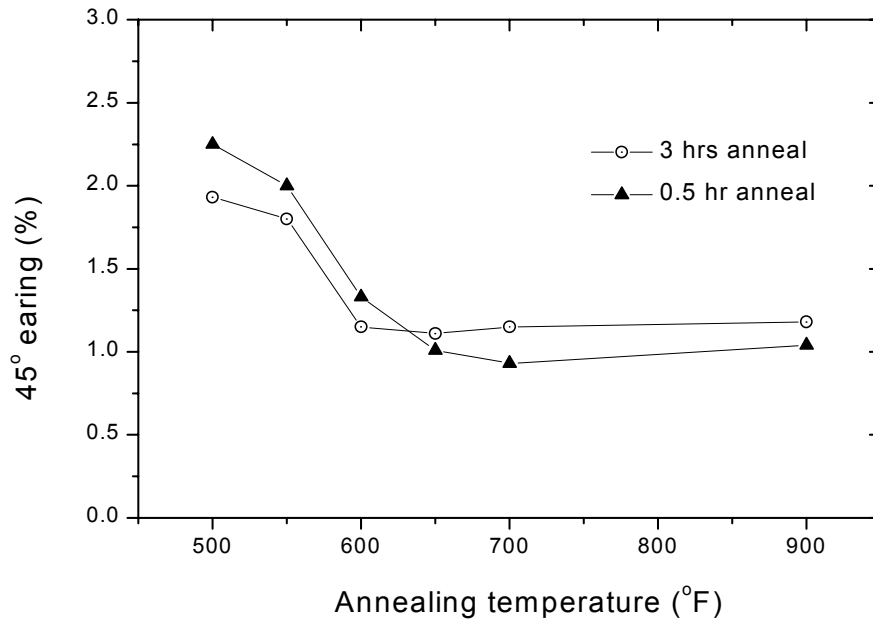


Fig. 22 Earing values after the 0.160” hot band homogenized at 900 °F in a salt bath for 3 hours and 0.5 hour respectively, cold rolled to 0.080” and annealed in a salt bath.

#### 4.2 University of Michigan: Effect of Cold Rolling on the properties of 5052 Al Sheet Produced by Continuous Casting

##### Summary

A study was performed to determine the role of cold rolling + annealing process on the properties of continuous cast and hot rolled sheet 5052 Al sheet. The tensile properties, microstructures and textures of 5052 Al sheets, 0.063" thick, from the two different process schedules were examined. One was as-received continuous cast sheet provided in hot rolled condition. The other was produced in the laboratory by cold rolling from a 0.125” thick sheet received from continuous cast and hot rolled condition. This sheet is referred to as the lab-processed sheet. Cold rolling and annealing improved tensile elongation and the values of  $n$  and  $R$  compared to the values for as-received continuous cast sheet. Laboratory TMT process produced finer grains compared to as-received sheet. With increase in reduction during cold rolling followed by annealing, shows that the laboratory process produces more random distribution of crystallite orientations and minimizes the intensity of cube component.

##### Experimental

Tensile specimens of size ASTM E8 (gauge length = 50.8mm) were cut along rolling direction and transverse direction. Then, all the tensile test specimens were annealed at 400°C for 90min, and air-cooled. This treatment was previously found to produce the lowest yield strength in the alloy, indicative of recrystallization-annealed condition. Uniaxial tensile tests were carried out in 5505 Instron tensile test instrument with crosshead velocity of 1mm/min and an extensometer with a gauge length of 50.8mm. The samples for optical microscopy were aged at 160°C for 15h after annealing treatment to cause precipitation to decorate the grain boundaries. The specimens were etched with Keller's reagent, and microstructures in the center and near the surface in the thickness direction of sheets were observed in Olympus PME3 optical microscopy.

Plastic anisotropy of the sheets are a direct reflection of crystallographic texture and is indicative of sheet drawability. This parameter, R, is defined as the ratio of width strain to thickness strain in the tensile specimen were determined from measurements of these strains from the tested specimens. It is defined as

$$R = \frac{\varepsilon_w}{\varepsilon_t}$$

where w and t refer to the width and thickness direction of the tensile specimen. Thus,  $\varepsilon_w = \ln(w/w_0)$  and  $\varepsilon_t = \ln(t/t_0)$ . However, because thickness strain,  $\varepsilon_t$ , cannot be accurately measured in a thin sheet, it is obtained from measurements of length and width strains far from the neck region, using volume constancy,  $\varepsilon_t = -(\varepsilon_l / \varepsilon_w)$ . The length strain,  $\varepsilon_l$ , can be obtained from  $\varepsilon_l = \ln(1 + \varepsilon_E)$ , where  $\varepsilon_E$  is the uniform strain.

The curves of engineering stress vs. engineering strain, and true stress vs. true strain were plotted using Kaleidagraph software. The values of strain hardening exponent, n, could be determined from the slope of the logarithmic plot of true stress vs. true strain. These plots exhibited two stage hardening behavior. The value of strength coefficient, K, is equal to the value of  $\sigma$  for  $\varepsilon = 1.0$ . These values were determined from each of the two segments of the curve.

Crystallographic textures were examined by determining the X-ray pole figures of (111) and (200) poles from both as-received sheet and lab-processed sheet using Computerized Rigaku diffraction system. It consists of a 12 kW high intensity rotating anode X-ray generator with a horizontal goniometer for powder work and a second goniometer with a pole figure attachment. 3/4" square specimens were cut from these sheets and annealed at 400°C for 90min for pole figure work. Then, the surfaces of specimens were polished in 120<sup>#</sup> sand paper and cleaned by acetone. The X-ray equipment was used with 40 kV voltage and 100 mA current.

## Results and Discussion

*Mechanical properties:* Table 1 summarizes the various mechanical properties of initial 5052 Al sheet with thicknesses of 0.125" and 0.063", produced by continuous casting process. These materials retained some amount of cold work as evidenced from their high yield strength of 265 MPa, and low elongation in the vicinity of 6-7%. Fig.1 shows plots of engineering stress vs. engineering strain for the as-received sheets, and Fig. 2 shows

logarithmic plots of true stress vs. true strain. The strain hardening exponent,  $n$ , and strength coefficient,  $K$ , can be determined from these plots. It can be found that all values of sheet with thickness of 0.125" are somewhat higher than that of sheet with thickness of 0.063" except for the value of  $R$ . The unusually low  $R$  values ( $\sim 0.2$ ) of these materials appear to be a consequence of hot rolling after continuous casting. These low  $R$  values may be a result of the banded microstructure consisting of low angle grain boundaries. These  $R$  values are much lower than those of materials conventionally prepared by cold rolling and annealing.

Table 1 Mechanical properties of 5052 Al initial sheet produced by continuous casting and hot rolling

| Material                  | Test direction | YS (MPa) | UTS (MPa) | El (%) | $n$  | $K$ (MPa) | $R$   |
|---------------------------|----------------|----------|-----------|--------|------|-----------|-------|
| As-received, (0.125" thk) | R.D.           | 264.5    | 328.0     | 6.8    | 0.04 | 323.1     | 0.245 |
| As-received, (0.063" thk) | R.D.           | 266.1    | 336.8     | 7.7    | 0.05 | 334.3     | 0.187 |

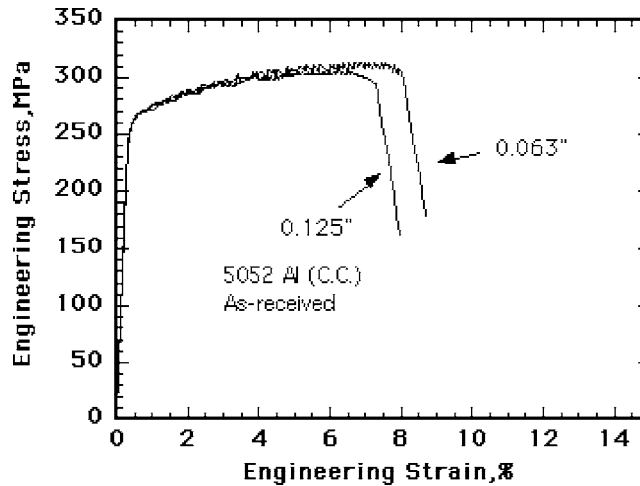


Fig.1 Curves of engineering stress-strain for continuous casting plates with thickness of 0.125" and 0.063"



It was also found that for the sheet cold rolled to 0.03" (from 0.125"), the mechanical properties were inferior compared to the properties of the 0.063" thick sheet, except for its higher R value. All of these materials exhibited a two-stage n-value behavior, and typically the 0.063" thick lab-processed material maintained a high  $n_2$  value.

Fig.3 is plots of engineering stress and strain for both of as received sheet and laboratory processed sheet. The stresses are a little bit higher in rolling direction than that in transverse direction at the same strain levels for as received sheet. However, the stresses are much higher in transverse direction than that in rolling direction for laboratory processed sheet.

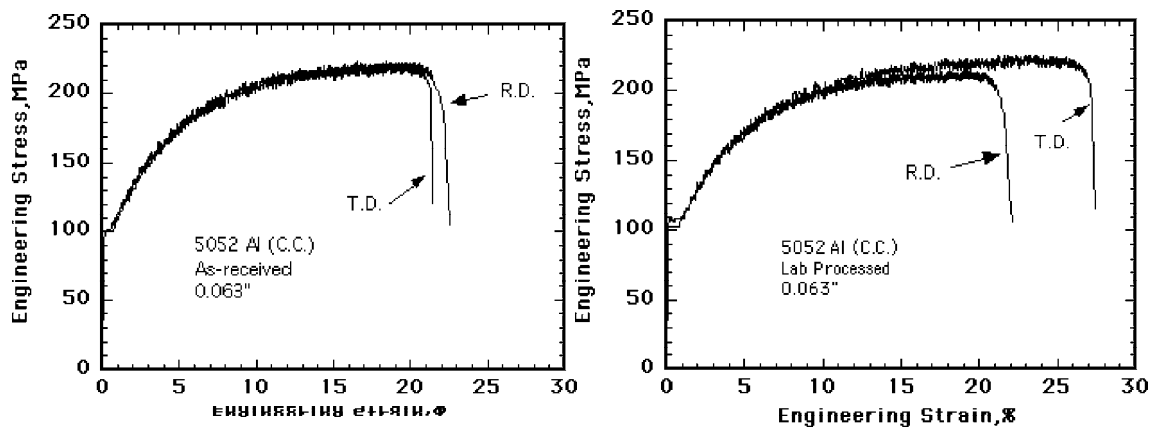
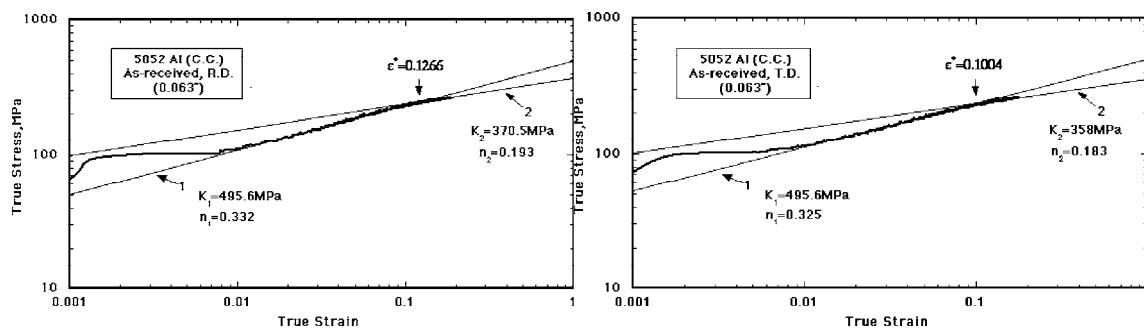


Fig.3 Curves of engineering stress-strain for both of as received sheet and laboratory processed sheet after annealing at 400<sup>0</sup>C for 90 min

Fig.4 is logarithmic plots of true stress and strain. Two stages work hardening is again observed. The terminal values of the strain hardening exponent,  $n_2$ , are substantially less than the earlier constant values in all plots.



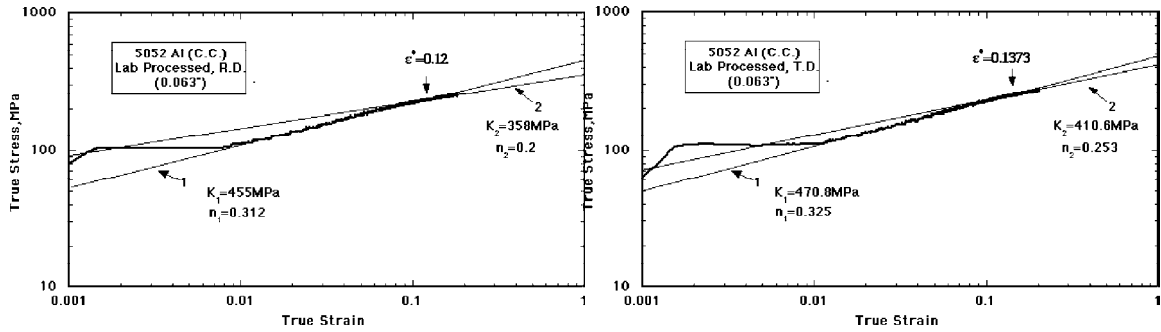
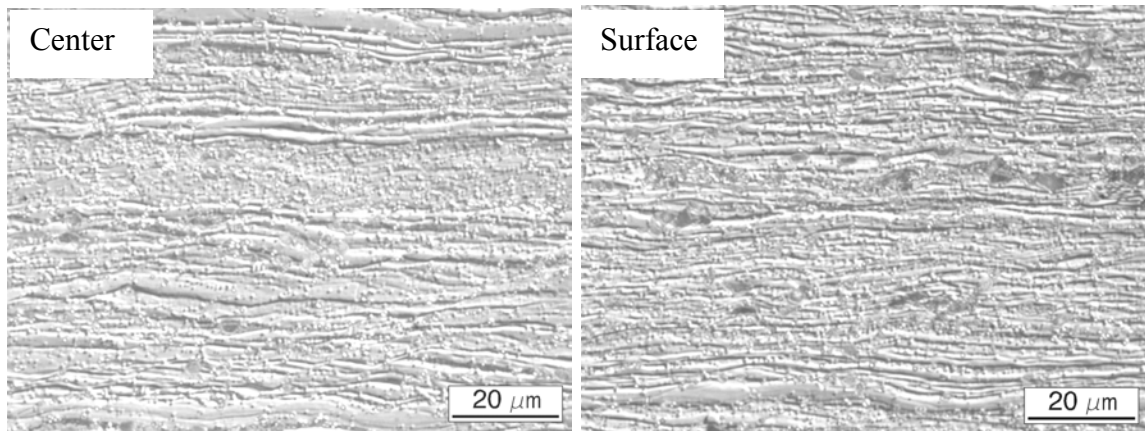


Fig.4 Curves of true stress-strain for both of as received sheet and laboratory processed sheet after annealing at 400°C for 90 min

### 1.1 Microstructure

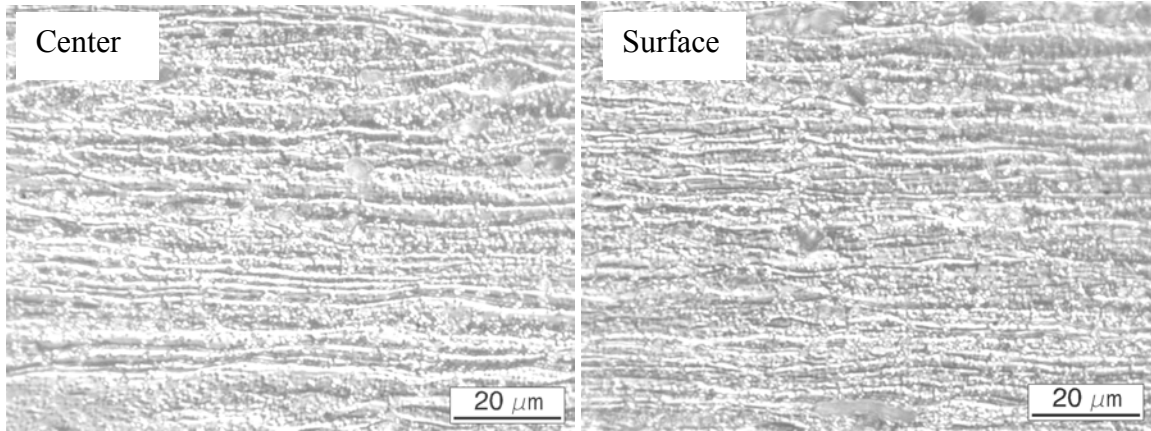
The microstructures of sheet cross-section containing the thickness direction and the rolling direction of both the as received specimens and laboratory processed specimen, from the center and surface of specimen are shown in Fig.5 and Fig.6. The grains near the surface are finer than that in the center for both specimens. In as received specimens, from near surface to center, the grain length reduces from 74.5µm to 47 µm, and the grain thickness from 2.65µm to 1.57µm. The grains in laboratory processed sheet are finer than that in same sections of as received sheet. The coarse grains in as-received sheet may be responsible for lower  $n_2$  value and higher R value compared to laboratory processed sheet.



(a) Microstructure in the center  
( $d_l = 74.5\mu\text{m}$ ,  $d_t = 2.65\mu\text{m}$ )

(b) Microstructure near the surface  
( $d_l = 47\mu\text{m}$ ,  $d_t = 1.57\mu\text{m}$ )

Fig.5 Microstructure in the thickness direction of 5052 Al sheet, thickness = 0.063", as received, (annealed at 400°C for 90min and aged at 160°C for 15h)



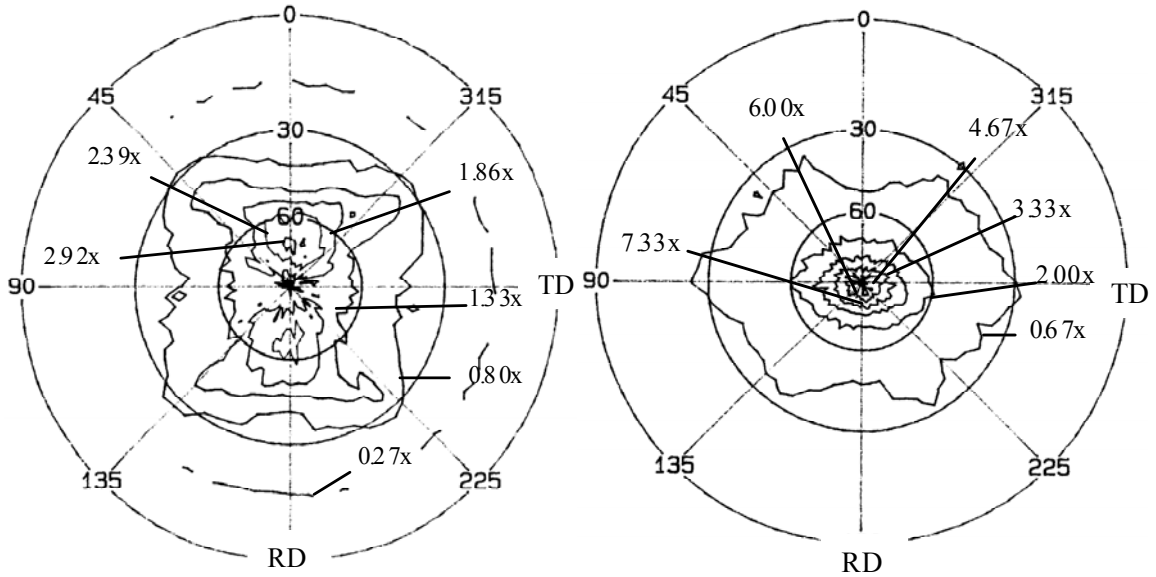
(a) Microstructure in the center  
( $d_l = 52.2\mu\text{m}$ ,  $d_t = 2.19\mu\text{m}$ )

(b) Microstructure near the surface  
( $d_l = 33.6\mu\text{m}$ ,  $d_t = 1.38\mu\text{m}$ )

Fig.6 Microstructure in the thickness direction of 5052 Al sheet, thickness = 0.063", lab processed, (cold rolled from 0.125" thk. and annealed at 400°C for 90min and aged at 160 °C for 15h)

## 1.2 Texture

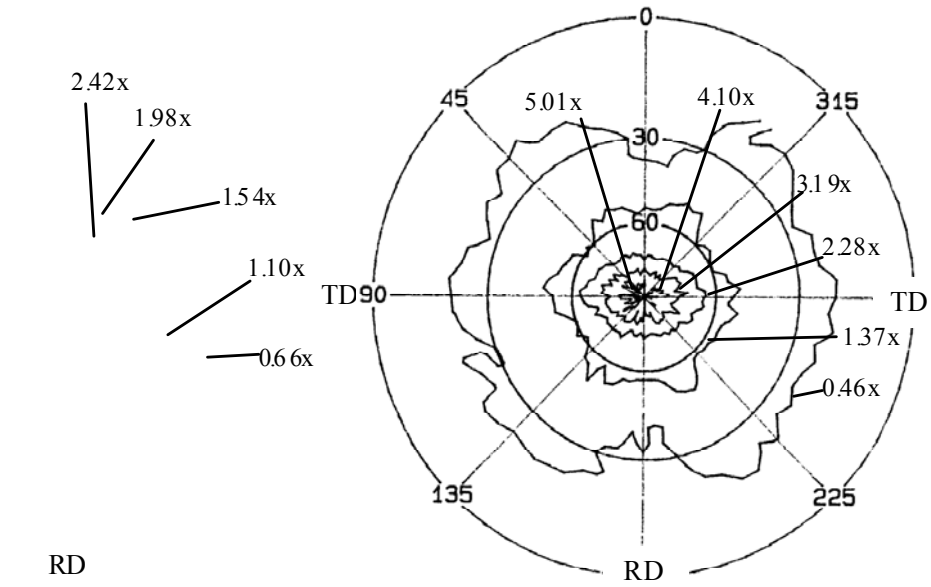
Crystallographic textures were examined by determining the X-ray (111) and (200) pole figures, shown in Fig.7, Fig.8 and Fig.9 for as received sheet, laboratory processed sheet with thickness of 0.063" and 0.03", respectively. The pole figures indicate a mixture of deformation and annealing textures. The pole intensities in the peak regions for (111) are around 3 times random for all sheets. However, the pole intensities in the peak regions for (200) are around 6-8 times random for as received sheet, 4-6 times random for laboratory processed sheet with thickness of 0.063", and 3-4 times random for laboratory processed sheet with thickness of 0.03". These results show that the laboratory cold rolling process reduces the fraction of cube texture, which may be related to its higher R value.



(a) (111)

(b) (200)

Fig.7 X-ray pole figures of 5052 aluminum sheet, as-received, 0.063" thk., (Annealed at 400°C for 90 min)



(a) (111)

(b) (200)

Fig.8 X-ray pole figures of 5052 aluminum sheet (C.C.), lab processed, 0.063" thk., (Cold rolled from 0.125" thk and annealed at 400°C/90 min)



There was initial difficulty in preparing specimens with high quality surfaces (finish and absence of damage) to produce EBSD patterns of sufficient clarity to permit rapid, automated analysis by the OIM system. Specimen quality was hampered both by the coarse oxide and intermetallic stringers and the deformed structure of the as-rolled material. However, a combined technique utilizing a final electropolish typical of the preparation of TEM specimens was developed. This technique successfully produces specimens with the prerequisite high quality surfaces for OIM. More than 40 OIM maps were acquired from a variety of material conditions, positions and orientations relative to the as-rolled material. Even at the  $\sim 0.8$  second per pixel acquisition speed of the current OIM system, the OIM maps required from 8 to 24 hours in order to acquire the high spatial resolution data needed for the modeling efforts.

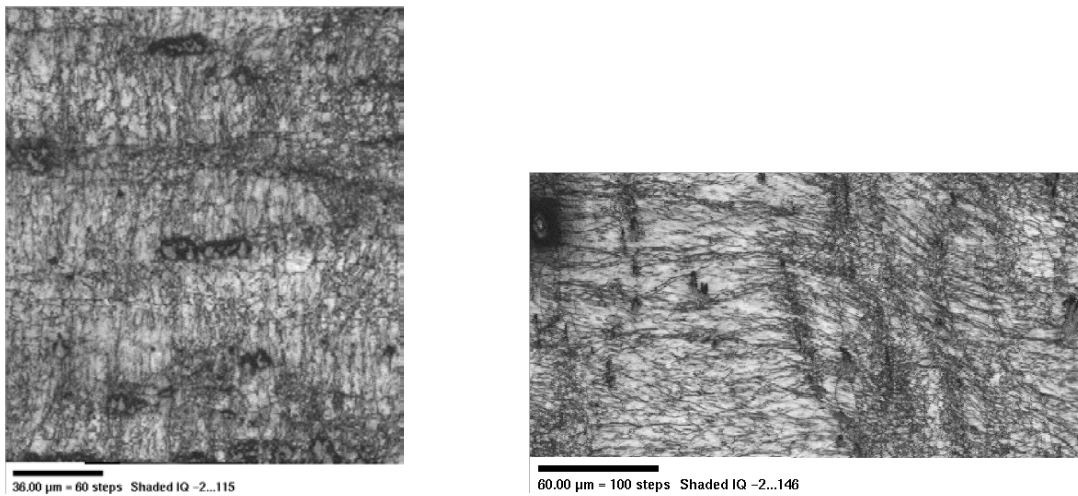


Figure A. Image quality map of alloy AA5754 hot band in the RD/TD surface (left) and RD/TD mid-thickness (right) planes.

The structure and microtexture of the as-rolled 0.08" 5754 hot band were examined as a function of depth in the sheet. Figure A compares the structure exhibited by image quality mapping at the surface and the midplane of the hot band in the RD/TD section. Dark bands indicate the presence of both grain and cell boundaries, as well as the coarse stringers of oxide and intermetallics. The midplane specimen was measured rotated  $90^\circ$  around the ND relative to the surface specimen.

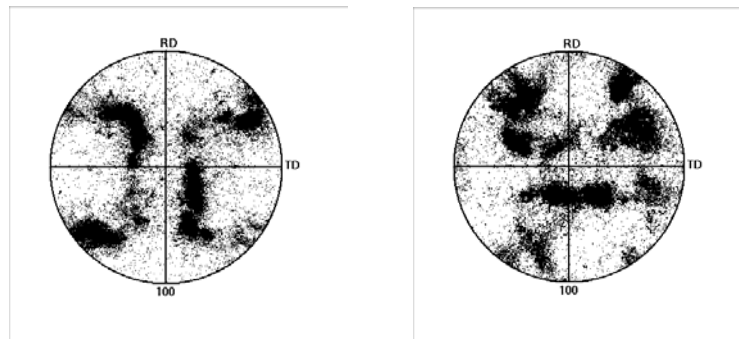


Figure B. (100) pole figures for the surface (left) and mid-thickness (right) for the images shown in Figure A.

The 001 pole figures shown in figure B for the two materials are similar, but not exact matches. This difference arises from the higher shear deformation in the near-surface region. There was little or no evidence for cube texture in these two measurements. However, there are areas in the as-rolled 5754 hot band that do exhibit small amounts of

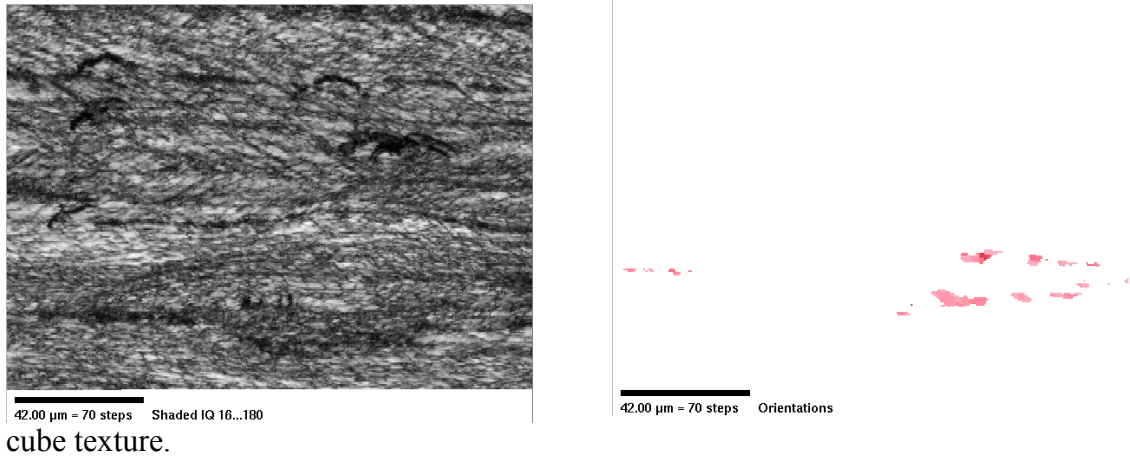
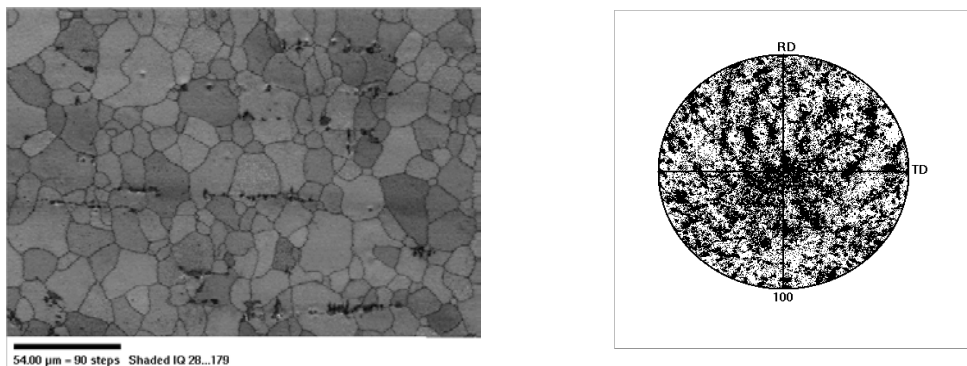


Figure C ND/TD midplane section showing the image quality map (left) and regions misoriented up to 10 deg. from cube orientation.

Figure C shows the mid-plane structure for the ND/TD section of the as-rolled material and the areas with orientations within  $10^\circ$  of the cube texture ( $\sim 0.7\%$  of the total area). These areas appear to be associated with the oxide/intermetallic stringers. It is possible that the local deformation and lattice rotation is inhomogeneous as the result of these hard



inclusions.

Figure D. RD/TD surface plane of 5754 flash annealed to 900F using plasma heating

In a similar fashion the structure and microtexture of the flash annealed ( $900^\circ\text{F}$ , 1 second) were determined by OIM. Figure D shows the structure and 001 pole figure for the RD/TD surface of the flashed annealed material, and Figure E shows the same for the RD/TD mid-plane of that material.

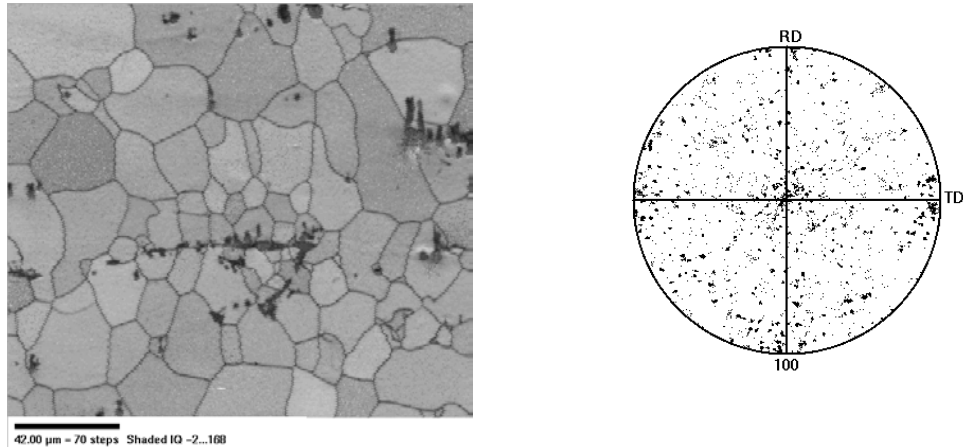
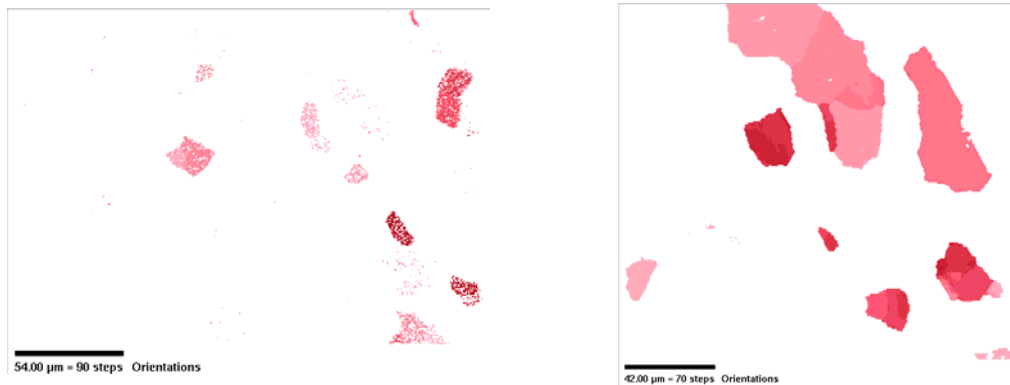


Figure E. RD/TD mid-thickness plane of 5754 flash annealed to 900F using plasma heating

Both regions exhibit roughly equi-axed grain structures indicative of recovery and recrystallization. The surface region has a predominantly random texture with only a small amount of cube texture (~3%); whereas the given midplane region exhibits significant cube texture (~19%). This difference between these two regions indicates a link to the inhomogeneous deformation state as a function of depth. The cube oriented grains for the two materials are presented in figure F. However, other regions of the midplane region exhibit lower presence of cube oriented grains (as low as 4%). These measurement indicate that the microtexture of the flash annealed material has some inhomogeneity on length scales greater than 200 microns. This inhomogeneity of the microtexture of the flashed annealed material may reflect an microtextural inhomogeneity in the as-rolled hot band or an inhomogeneity in the stringer distribution (e.g., the intermetallics and their distribution may be impacting the recovery and recrystallization



during the flash annealing.

Figure F. Cube oriented regions in the RD/TD surface plane (left) and RD/TD mid-thickness plane (right) of flash annealed 5754 hot band.

The dislocation and fine precipitate structures of both the as-rolled and flash annealed 5754 hot band have been investigated by TEM. As expected both the near-surface and

midplane regions of the as-rolled material exhibit fine cell sizes (<2 micron) and significant intercellular dislocation structure (dislocations and low angle walls). The flash annealed materials exhibited a large grain size consistent with recrystallization. However, a significant dislocation substructure that included dislocation dipoles and loops was present. This observation differs from the very low dislocation density observed in conventionally annealed materials and may reflect a difference in the recovery/recrystallization process in flash annealed material. There may be insufficient time during the rapid cool down to permit complete removal of the dislocation structure.

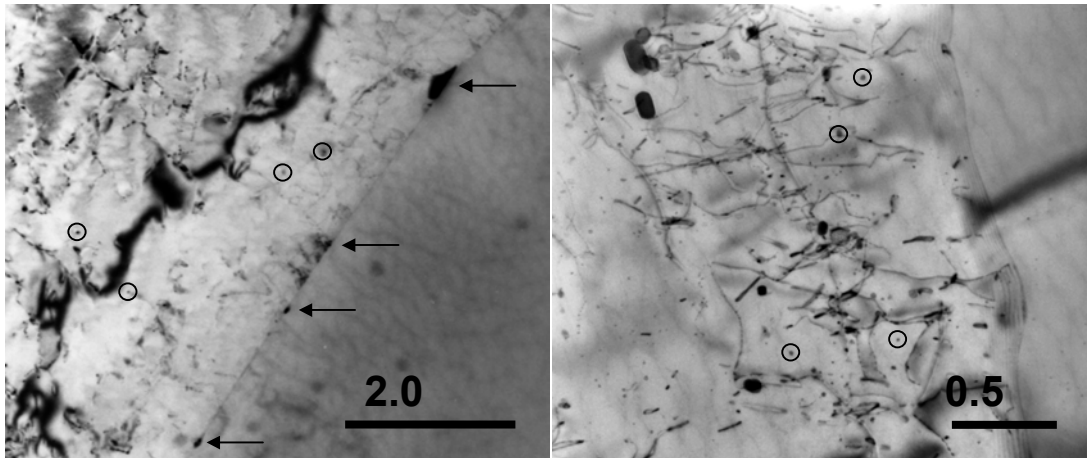


Figure G. TEM images of 5754 hot band annealed at 900F, 1s at the RD-TD mid-thickness plane (left) and RD-TD surface plane (right). Arrows indicate GB precipitates and circles indicate some fine matrix precipitates. In the right image the elongated loop-like images are dislocation dipoles and loops

Fine (<500 nm) precipitates were present both in the matrix and on grain boundaries in the flash annealed material shown in figure G. X-ray microanalysis of both types of precipitates showed enrichment in Mn and Fe indicating that they are intermetallics rather than the oxides. It is possible that the presence of these fine precipitates would affect the recrystallization kinetics of the hot band.

#### 4.3.2 High temperature mechanical properties of 5052 hot band

Compressive stress-strain behavior was investigated for 0.875-in thick slab of 5052 aluminum (cast no. 5324) received in the as-cast condition from Commonwealth Aluminum (Newport Rolling Mill #1). The purpose of this task effort was to formulate a compressive stress-strain relation of the material for simulation studies of rolling process and studies of changes in microstructure during the first pass.

A batch of twelve cylindrical specimens having a 0.4-in diameter and a small batch of three having a 0.5-in diameter were used. All the specimens are 0.85-in. Tests were done at five temperatures, ranging from 700 to 1100°F at a 100°F interval, and at three strain rates of 0.04, 0.4, and 4 in/in/min. All tests were discontinued when the specimens were compressed to about half of the initial length, simulating the first pass.

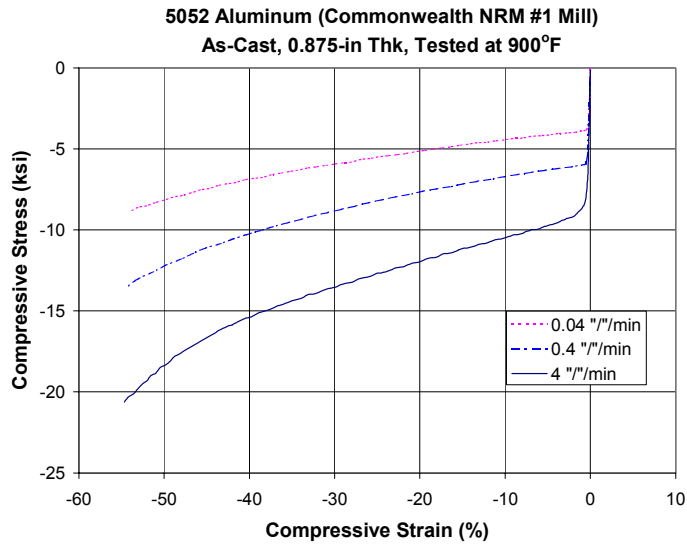


Fig 1 – Compressive engineering stress-strain curves of 5052 aluminum tested at 900°F.

A typical compressive stress-strain behavior (in the engineering stress-strain scale) at 900°F is shown in Fig 1. It shows the yield strength at the temperature is sensitive to the strain rate, the behavior known as viscoplastic effect. Although not shown here, the viscoplastic behavior was exhibited at all temperature levels tested.

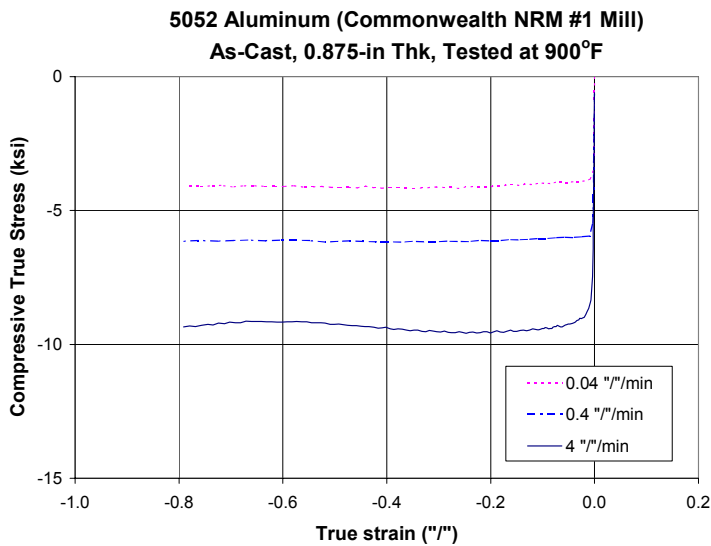


Fig 2 – True stress-strain description of same curves plotted in Fig 1

Figure 2 shows the same stress-strain behavior in the true stress-strain representation, with the customary assumption that cylinder remain cylinder during compression loading. As a result, the material showed to have behaved as a perfectly plastic solid. However, the true stress used in behavior modeling is based on the minimum diameter of the compressed specimen. A bilinear stress-strain relation with the true stress as a function of temperature and strain rate was recommended for the simulation study of rolling process.

Because of the space limitation, only the bilinear stress-strain curves at 800 and 900°F are illustrated in Fig 3.

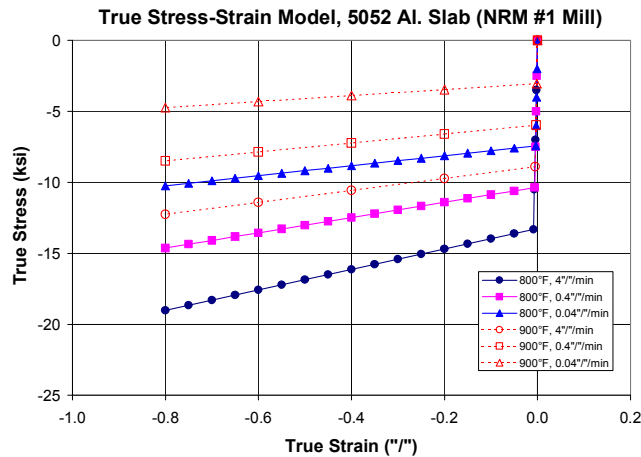


Fig 3 – Stress-strain behavior model of 5052 aluminum for simulation studies of rolling process

#### 4.3.3 Rapid Annealing Techniques for Production of Laboratory Samples

4.3.3 1. Gleeble Studies: The purpose of this effort was to determine whether the Gleeble thermo-mechanical simulator could be used to heat coupons of hot-band at the required rate of 500F to 900F in 0.75 seconds, so that a convenient alternative method of rapid heating for laboratory studies of microstructure and texture evolution during rapid heating could be established. The Gleeble thermo-mechanical simulator uses samples in the form of strips 6” long and 1” wide. The sample is gripped in water-cooled copper jaws at its ends with a gauge-length of roughly 2” between the jaws. The copper jaws and the sample form the secondary of a transformer and resistance heated by passing current through the sample. The power to the sample is controlled by a thermocouple which is spot welded to the midpoint of the gauge length. The thermocouple provides feedback control by sensing the difference between the sample temperature and a program temperature. Initial experiments using the Gleeble for heating a 0.080” thick AA5754 CC hot band were quite successful. Samples could be heated from 500F to 900F in 0.75 seconds without overheating the samples. Tensile testing of the Gleeble samples after thermal cycling showed a roughly 50% reduction in yield strength compared to the as-received, indicating significant microstructural change. However, the elongation to failure was lower than that of the as-received hot band, because of the presence of the Type-K thermocouple junction that was spot welded to the sample and the alloying between the thermocouple junction and aluminum sheet during the thermal cycle.

Further experiments were conducted using the Gleeble with the thermocouples welded away from the center-line of the samples such that the welds could be removed after Gleeble testing. Tensile testing of the Gleeble samples showed both significant softening as in the previous trials with a roughly 50% reduction in yield strength and a much improved tensile elongation compared to the previous samples that contained the

thermocouple welds. The tensile elongation in the rolling direction increased from about 12% for the as-received sample to about 14% in the heat treated sample. However, there was a sample-to-sample variability of about 2% for the Gleeble samples. The tensile elongation in the transverse direction increased significantly from about 10% for the as-received samples to about 14% for the Gleeble samples.

#### 4.3.3.2 Plasma Heating

Two infrared processing facilities at the Oak Ridge National Laboratory (ORNL) were used to produce a variety of transient heating profiles in aluminum test samples. The time/temperature histories produced in these samples were able to simulate the characteristics of a new continuous casting industrial process for producing rolled sheet materials. In the new process, induction heating will provide a capability to anneal the just rolled sheet as it exits the rolling mill.

Infrared process heating techniques were chosen for the simulation because of the relative simplicity of achieving experimental precision over the wide range of heating rates required to match the in-line annealing requirements. For example, the industrial requirements for providing in-line anneal processing of the sheet, as it exits, the rolling mill at 120 cm/s requires heating rates as high as 300°C/s. In order to match these very rapid heating rates, a plasma arc lamp system at ORNL was used and found to be very effective in preparing various types of metallurgical specimens.

In addition to the plasma arc lamp, another ORNL infrared system (quartz halogen lamp cylindrical furnace) has proved to be a useful tool in annealing the large number of samples required to benchmark the recrystallization modeling efforts, which are part of this project. This furnace is capable of moderately high heating rates, 25°C/s, and has a very uniform sample heating capability. The furnace is designed with highly reflective walls that are water-cooled. This feature provides rapid response feedback of the sample temperature to the furnace temperature controller.

*Experimental Facilities:* In order to prepare flash anneal samples at the required rapid heating rates, a 300-kW plasma arc lamp was utilized to produce tensile, earring, and metallography specimens. The capability of this system to anneal several millimeter-thick samples of aluminum is in excess of 1000°C/s. Shown schematically in Figure 1 are the basic attributes of the arc lamp.

Arc lamp sources are configured as a simple quartz tube, 4 cm ID, into which a mixture of dematerialized water and argon are injected (see Figure 1). The mixture is injected tangentially into the quartz tube's interior at one end of the tube. The resultant helical flow down the length of the tube produces a thin film of water against the tube wall, which effectively cools it. The argon gas flows in a similar fashion down the core of the tube and provides the medium into which a high-pressure plasma arc can be formed for passing up to 1200 A. These sources are able to operate continuously for up to 1000 h. Power output is continuously variable from near 1 kW to full power and requires only 0.020 s to ramp up or extinguish.

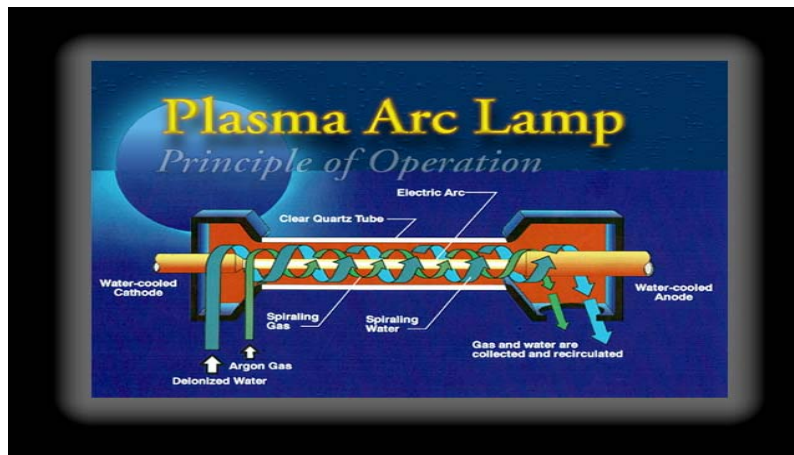


Figure 1. Schematic of an operational plasma arc lamp

For high power density process heating applications, a suitably designed water-cooled reflector is located around the quartz plasma arc tube as shown in Figure 2. A typical system operating at 300 kW in this configuration would be able to focus a beam over a 2- by 10-cm area at power densities of 3500 W/cm<sup>2</sup>.

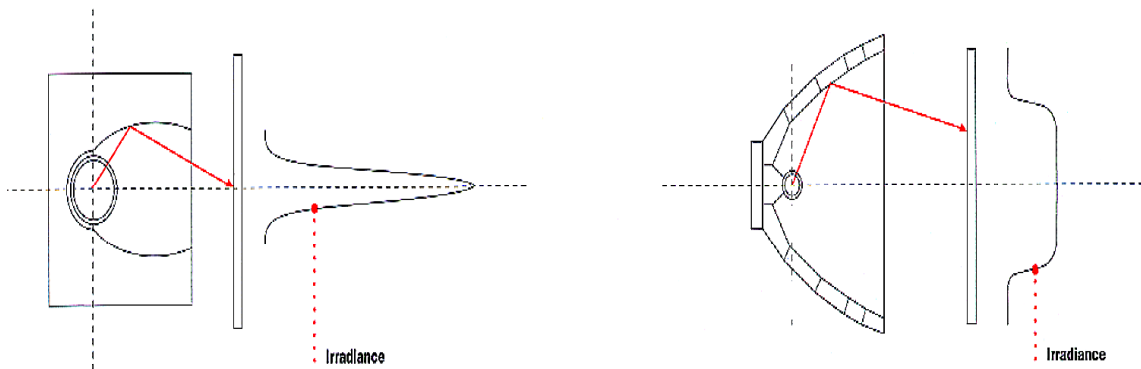


Figure 2. Arc lamp reflector configurations.

Other reflectors are available at our Plasma Arc Lamp Facility that provides focused rectangular beam profiles measuring: 3 cm by 20 cm and 3 cm by 35 cm, which produce power densities of 1200 W/cm<sup>2</sup> and 600 W/cm<sup>2</sup>, respectively. A uniform irradiance reflector shown in Figure 2 (right), will provide a uniform focus over a 20 cm by 20 cm area at 200 W/cm<sup>2</sup>.

Figure 3 shows a plan view of the Plasma Arc Lamp Facility at ORNL. Also shown is a close-up of the lamp mounted on a six-axis Cincinnati-Milacron model T3-776 robot. A Universal Robot Controller (URC) developed and built by Robot Workspace Technologies, provides precise positioning and scanning capability for the arc lamp head. Using the robot in conjunction with the plasma arc lamp greatly increases the facility's

flexibility for performing a variety of experiments. There are also a variety of processing boxes available for the heating of specimens in different atmospheres when using the plasma arc lamp.

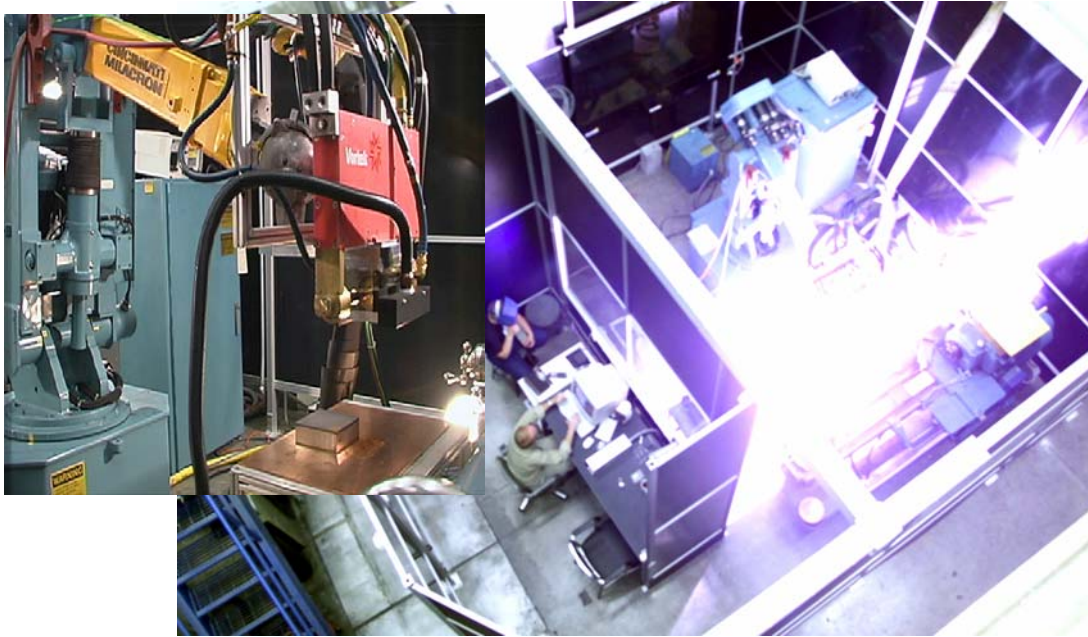


Figure 3. Plasma Arc Lamp Facility

The facility work cell is designed with safety interlocks on the door and pass through, cutting off the lamp instantaneously if somebody inadvertently tries to enter the cell while the arc lamp is on. Retractable welding curtains on the side windows are interlocked so that they must be down before the lamp can be started. Also, the work cell is interlocked by infrared beams that shut down operation if the robot should leave its predetermined work area, or if something should inadvertently enter the cell during processing.

On-line video monitoring is available for video recording of experiments from different locations inside the enclosure. PC-based data acquisition is used in the facility and allows for automated temperature, heat flux, and lamp head position/kinematics to be monitored during processing.

For specimens that required heating rates less than  $25^{\circ}\text{C/s}$ , a 33-kW cylindrical furnace configured with quartz halogen heating lamps provided a very precise and rapid method for uniformly heating samples larger than the region of uniform focus in the plasma lamp. The furnace is shown in Figure 4.



Figure 4. A 33-kW, tungsten halogen cylindrical furnace

The cylindrical infrared furnace utilizes a tight packed circular array of 165-mm-long tungsten halogen lamps. The lamp filaments operate in excess of 2800°C, providing a very high power density capability. The filaments are individually enclosed in quartz tubes, which have an operating temperature capability of 1100°C. The lamps can be cycled from cold to full emission in 0.75 s. Shutdown times are almost identical. The furnace is PID/fuzzy logic controlled, which allows for precise processing schedules.

Inside the lamp array, an optional 92-mm-ID by 73-mm-long quartz tube can be provided as a transparent containment vessel for processing in various atmospheres, including vacuum 10-m Torr max. The furnace's hot zone can accommodate a rectangular sample sized, 82-mm wide × 57-mm high × 152-mm long.

*Sample Preparation:* All samples that have been processed to this point in the project have been made from one material. That is, 5754 Al, which was rolled at the Carson Mill to a thickness of 2 mm (0.080 in.). From this material, four different sized samples were fabricated to accomplish the different tasks of: (1) 20-cm plasma lamp, flash annealing of tensile specimens (14 cm × 2 cm × 2 mm); (2) 10-cm plasma lamp, flash annealing of tensile specimens (10 cm × 1 cm × 2 mm); (3) 10-cm plasma lamp, flash annealing of earring samples (7.6 cm × 7.6 cm × 2 mm); and (4) 33-kW cylindrical infrared furnace, flash annealing of modeling benchmark samples (12.4 cm × 2 cm × 2 mm).

For each group of samples, it was necessary to attach multiple type K thermocouples to dummy specimens that were identical to the actual samples. These dummy specimens were used to develop heating profile parameters for the plasma arc lamp or cylindrical infrared furnace. Once the heating profiles (power and exposure duration) were developed for a given anneal cycle, samples could be annealed without changing the material that was being tested by the attachment of a thermal couple. An example would be the gauge section of tensile specimen.

Thermocouples were attached to dummy specimens by making a shallow depression in the sample with a sharp wood chisel. The small 3-mm-long depression produced in this manner had raised sides into which a thermocouple junction was placed and subsequently panned shut. This method of attachment was superior to the more conventional method of spot welding for several reasons. It was found that the spot welding to the 5754 Al produced a very brittle junction, which often fell off during subsequent handling. In addition, spot welding often produces an obvious large change to the surface emissivity of the sample. Since these samples are heated by the surface absorption of infrared, having a nonuniform surface emissivity, will introduce sample temperature measurement errors. The photograph in Figure 5 shows a 10-cm-long dummy tensile specimen with a single attached thermocouple. Figure 6 shows the specimen installed in the plasma arc lamp processing chamber, prior to profile development runs.

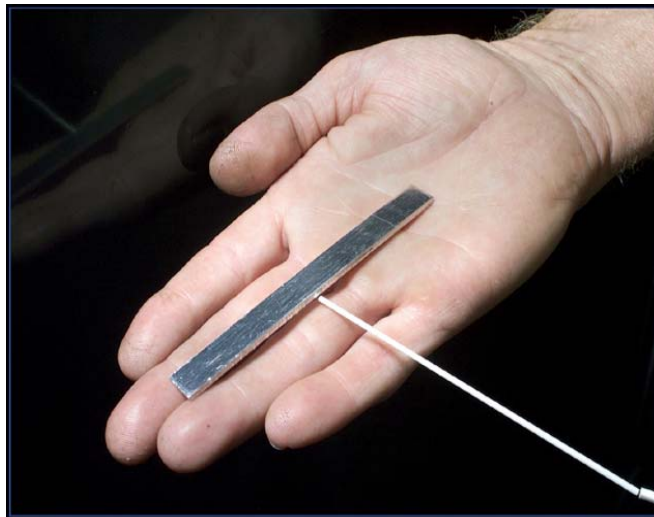


Figure 5. 5754 aluminum, dummy tensile specimen for determining the flash anneal power/time profile when exposed to the 10-cm plasma arc lamp at the Oak Ridge National Laboratory, Oak Ridge, TN.

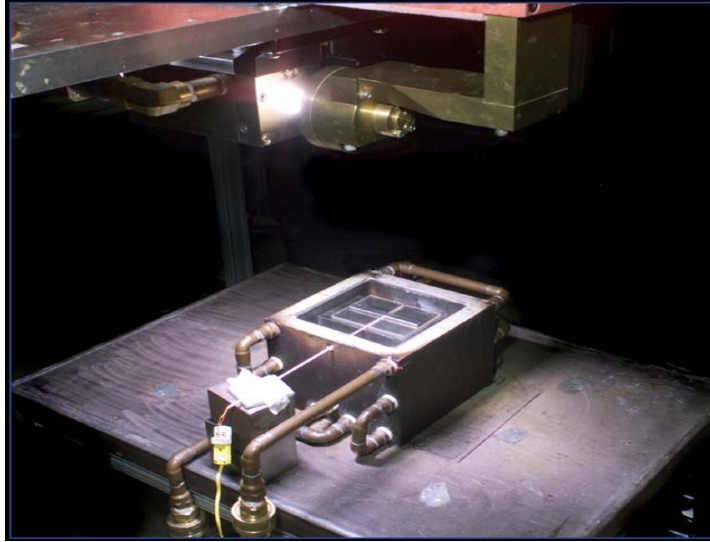


Figure 6. 5754 aluminum, dummy tensile specimen installed in the processing box prior to anneal profiling by the 10-cm plasma arc lamp at the Oak Ridge National Laboratory, Oak Ridge, TN.

### *Infrared Processing*

#### *Initial, 20-cm plasma arc lamp flash annealing of Alloy 5754 aluminum tensile specimens*

Based on the processing requirements for the Carson Mill industrial trials for the induction heating, in-line-anneal process, an initial series of experimental tasks were outlined for developing a more precise understanding of rapid annealing by using the infrared facilities at ORNL. These tasks were mutually agreed upon by the various team members and were designed to support the industrial demonstrations that would take place at the Carson Mill during February 2002.

The first task that was devised for examination by infrared processing was to simulate mill-heating profiles that would occur in the continuous-cast hot band as it exits in the rolling mill at 260°C and is induction heated to a higher temperature at mill speed (i.e., 120 cm/s for 2-mm sheet). The length of the induction heating apparatus in the rolling direction is about 120 cm and therefore about 1 s of heating time is the interval during which the heating system must increase the temperature of the throughput material. Temperatures of interest to the team were 372°C (700°F), 472°C (800°F), and 482°C (900°F).

The size of the samples was determined by the need to perform standard tensile testing on the annealed specimens and by the area that the focused infrared beam could uniformly heat a sample. The sample size that satisfied both criteria was 14-cm long × 2-cm wide × 2-mm thick. This size sample fits well within the focus of the 20-cm arc lamp by allowing misalignment margins of 0.5 cm on the width and 3 cm on the ends. In addition,

the size was convenient for making standard tensile specimens from the annealed sheet specimens.

Shown in Figure 7 is a typical temperature response for one of the above-described tensile specimens processed with the 20-cm plasma arc lamp. The anneal simulations were performed with the plasma lamp head in a stationary position above the sample, and the lamp power was programmed to heat the sample to 260°C over a 30-s interval and then increased to achieve the desired flash anneal temperature in 1 s. As described in the previous section, no thermal couple instrumentation was attached to the actual specimens that were used for tensile tests. Heating, power/time/ specimen position, and parameters were determined with separate instrumented samples until a repeatable temperature response was achieved. New specimens were then annealed with this profile for use in the appropriate metallurgical tests.

In the initial series of 1-s flash anneals performed with the 20-cm plasma arc lamp, microscopic examination of the annealed samples at 372°C (700°F), 472°C (800°F), and 482°C (900°F) revealed little if any recrystallization of the initial rolled structure, even at the 482°C temperature.

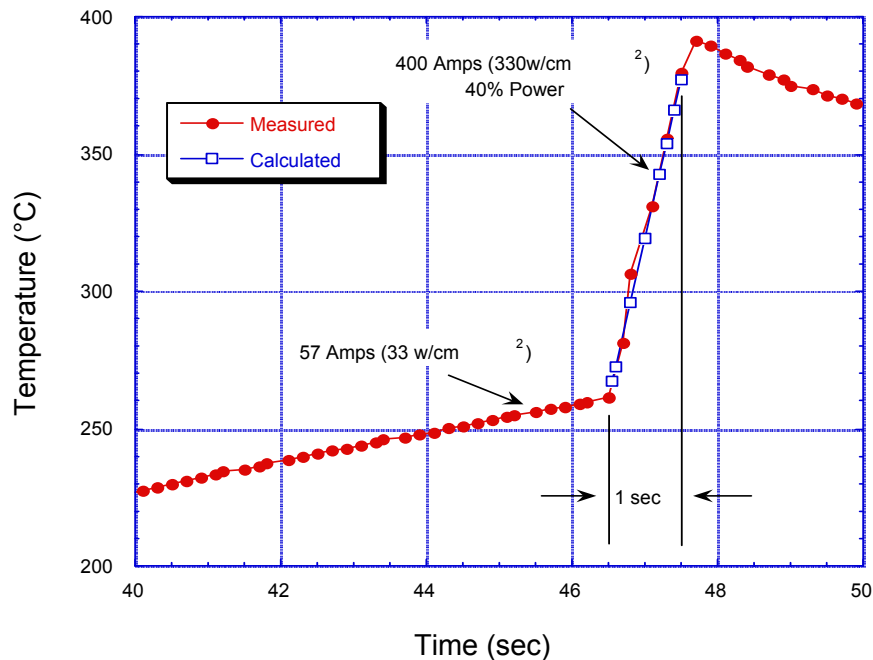


Figure 7. Typical temperature response for a 14-cm-long  $\times$  2-cm-wide  $\times$  2-mm-thick flash-annealed tensile specimen processed by the 20-cm plasma arc lamp.

*Continued flash annealing of rolled, 5754 Al tensile specimens with the 10-cm plasma arc lamp*

After review of the initial specimen experiments, it became clear that higher temperature flash anneal cycles would be required to achieve complete recrystallization of the Carson Mill 5754 Al rolled material. In addition, procurement delays in replacing the electrodes in the 20-cm arc lamp head necessitated that the new experiments be performed with the 10-cm arc lamp. Because of this, the tensile specimen sample size was changed to 10-cm long  $\times$  1-cm wide  $\times$  2-mm thick. The 10-cm arc lamp has almost three times the power density capability ( $3500 \text{ W/cm}^2$ ) as the 20-cm arc lamp and was therefore positioned in a defocused mode above the sample for all tests.

In this series of tests with the 10-cm lamp, the flash anneal series at  $372^\circ\text{C}$  ( $700^\circ\text{F}$ ),  $427^\circ\text{C}$  ( $800^\circ\text{F}$ ), and  $482^\circ\text{C}$  ( $900^\circ\text{F}$ ) was repeated with the new sized specimens. In addition, a new series was added [ $510^\circ\text{C}$  ( $950^\circ\text{F}$ ),  $537^\circ\text{C}$  ( $1000^\circ\text{F}$ ), and  $565^\circ\text{C}$  ( $1050^\circ\text{F}$ )]. The flash-anneal cycle temperature response plots for this 10-cm arc lamp series is shown in Figure 9. The micrographs that were made for the  $510^\circ\text{C}$  ( $950^\circ\text{F}$ ),  $537^\circ\text{C}$  ( $1000^\circ\text{F}$ ), and  $565^\circ\text{C}$  ( $1050^\circ\text{F}$ ) temperature series are shown in Figure 10 and clearly indicate that complete recrystallization has occurred at all three higher temperatures.

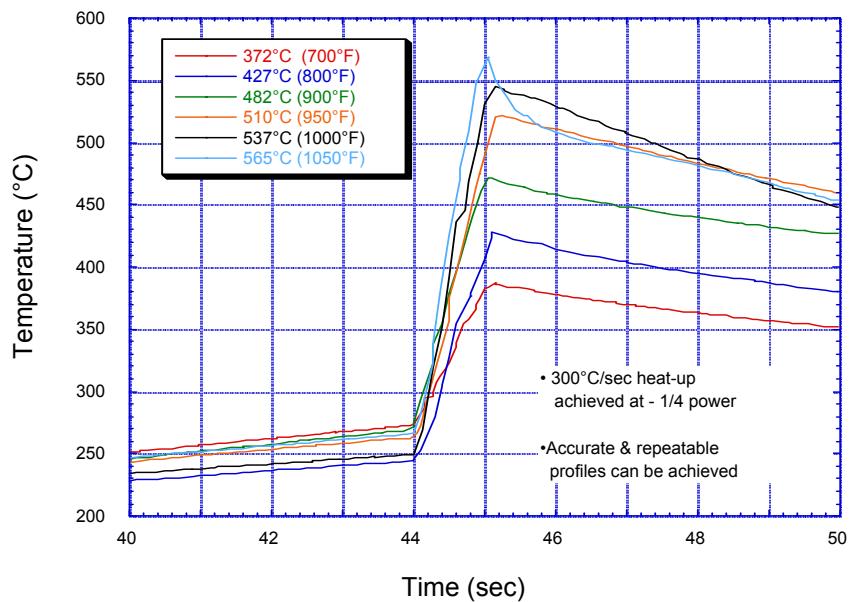


Figure 9. Typical temperature responses for a 10-cm-long  $\times$  1-cm-wide  $\times$  2-mm-thick flash-annealed tensile specimen processed by the 10-cm plasma arc lamp.

*Flash annealing of rolled 5754 Al earring specimens with the 10-cm-long focal length plasma arc lamp*

Discussions with project team members concerning the results of the above tensile specimen annealing results precipitated an interest in preparing a series of earring samples with the plasma arc lamp. These earring samples are large ( $7.6 \text{ cm} \times 7.6 \text{ cm} \times 2 \text{ mm}$ ), compared to the focus spot size of the arc lamps and would therefore have to be scanned by the beam.

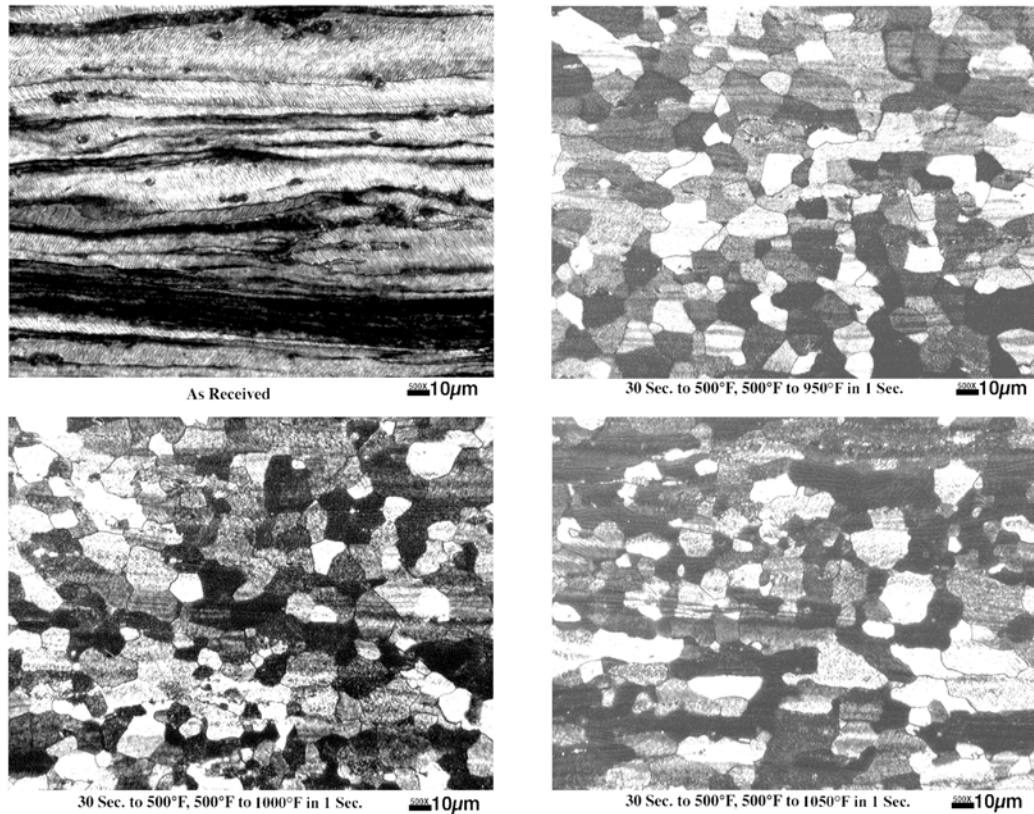


Figure 10. Microstructure of 10-cm plasma arc lamp flash annealed, 5754 Al at 510°C (950°F), 537°C (1000°F), and 565°C (1050°F). As-received rolled structure has been completely recrystallized

When scanning high thermal diffusivity material such as aluminum, there is considerable thermal conduction that occurs in the scan direction for cases where the beam profile is uniform across the width of the plate. This effect requires that the scan rate be slower at the start of the scan and faster towards the end of the scan if a uniform temperature rise at all portions of the sample is to be realized. This situation can be quantified by numerical modeling codes but was judged too time consuming compared to a more empirical approach, at least for the present goal of producing several test plates.

The power/scan rate profile that was developed for preparation of flash annealed earring samples was accomplished by attaching three thermal couples to the plate sample, along the scan direction at the: leading edge, mid-span and trailing edge. By monitoring these temperatures as the lamp was scanned, at constant power and increasing speed, the plate profile was developed and is shown in Figure 11. The temperature response of the rolled 5754 Al specimen scanned with this profile is shown in Figure 12.

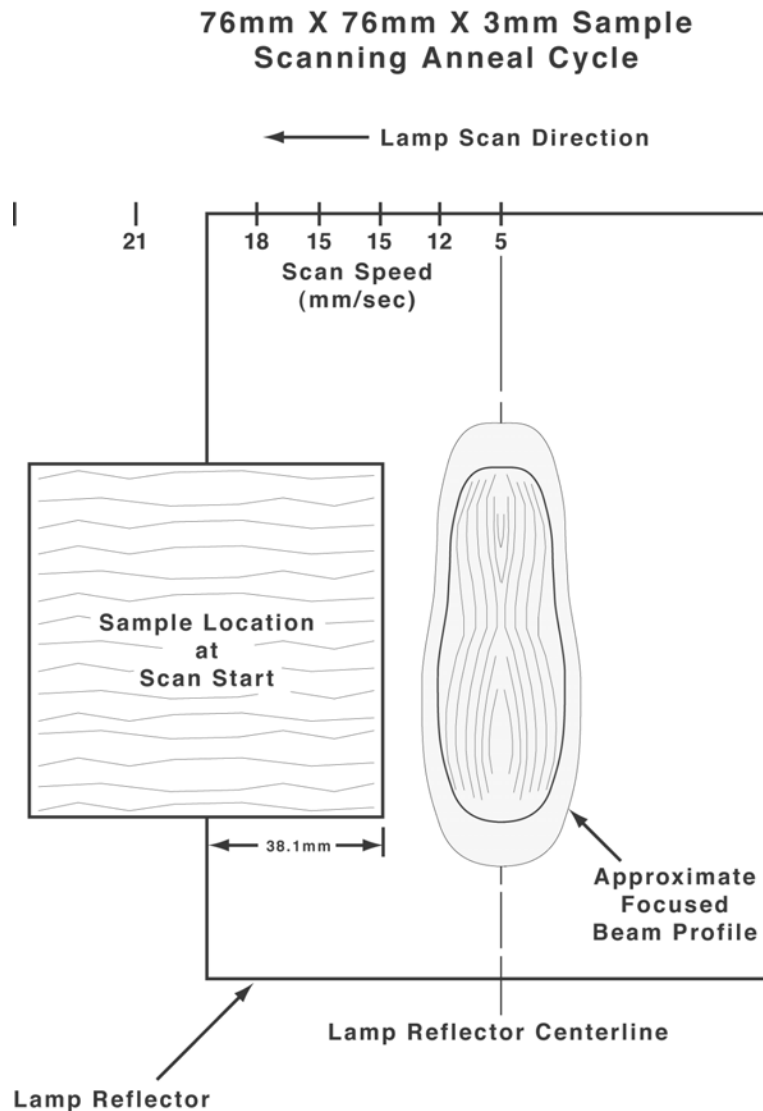


Figure 11. Variable scan rate profile for plasma arc lamp flash annealing of 7.6-cm × 7.6-cm × 2-mm earring specimens.

Metallography specimens were extracted from the plate that was scanned with this profile and is shown in Figure 13. The recrystallized grain structure, which occurred, was uniform across the plate except at the center (lowest temperature) and is shown in Figure 14. Ongoing work is in progress to improve this profile, which will probably eliminate the low temperature at the plate center.

*Modeling benchmark samples processed in the 33-kW tungsten halogen cylindrical furnace*

In order to support the modeling efforts rapid anneal samples were prepared in the 33-kW tungsten halogen cylindrical furnace. These samples were all annealed by rapidly increasing their temperature from ambient to 385, 427, 443, 460, and 471°C in 20 s. At each temperature, the samples were held for different intervals of time up to 32 min.

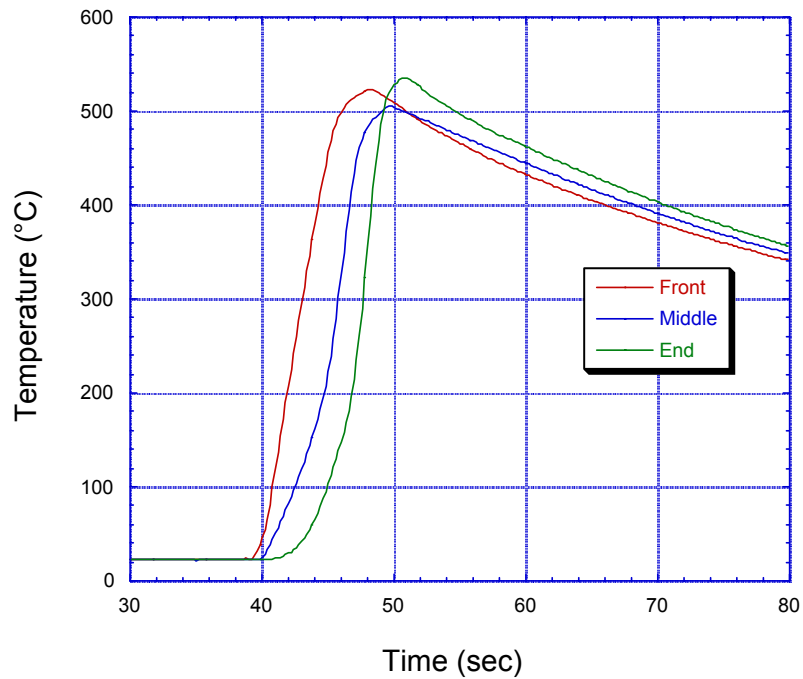


Figure 12. Temperature response of the rolled 5754 Al specimen scanned with the power/rate profile shown in Figure 11.

# 76mm X 76mm X 3mm Sample Metallography Specimens Map

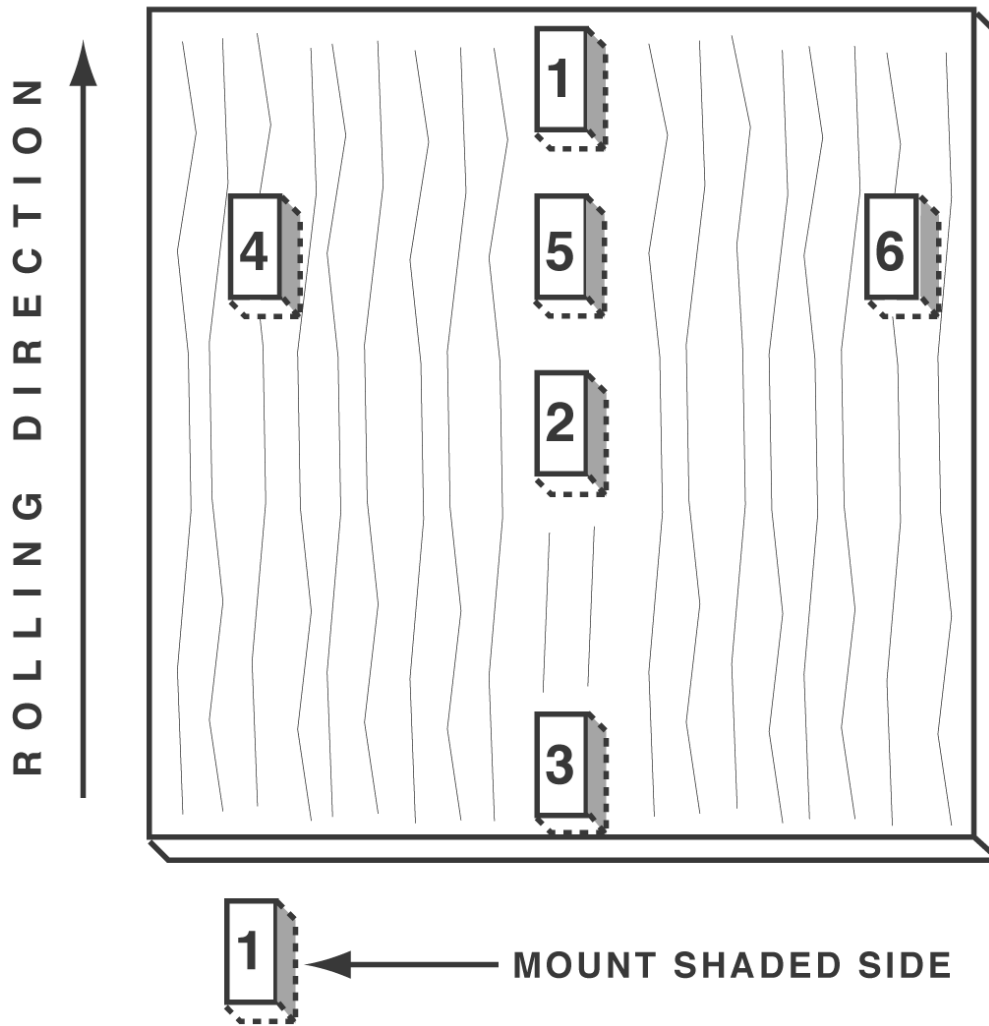


Figure 13. Metallography sample map of the rolled 5754 Al earring specimen that was plasma arc flash annealed to the profile shown in Figure 11

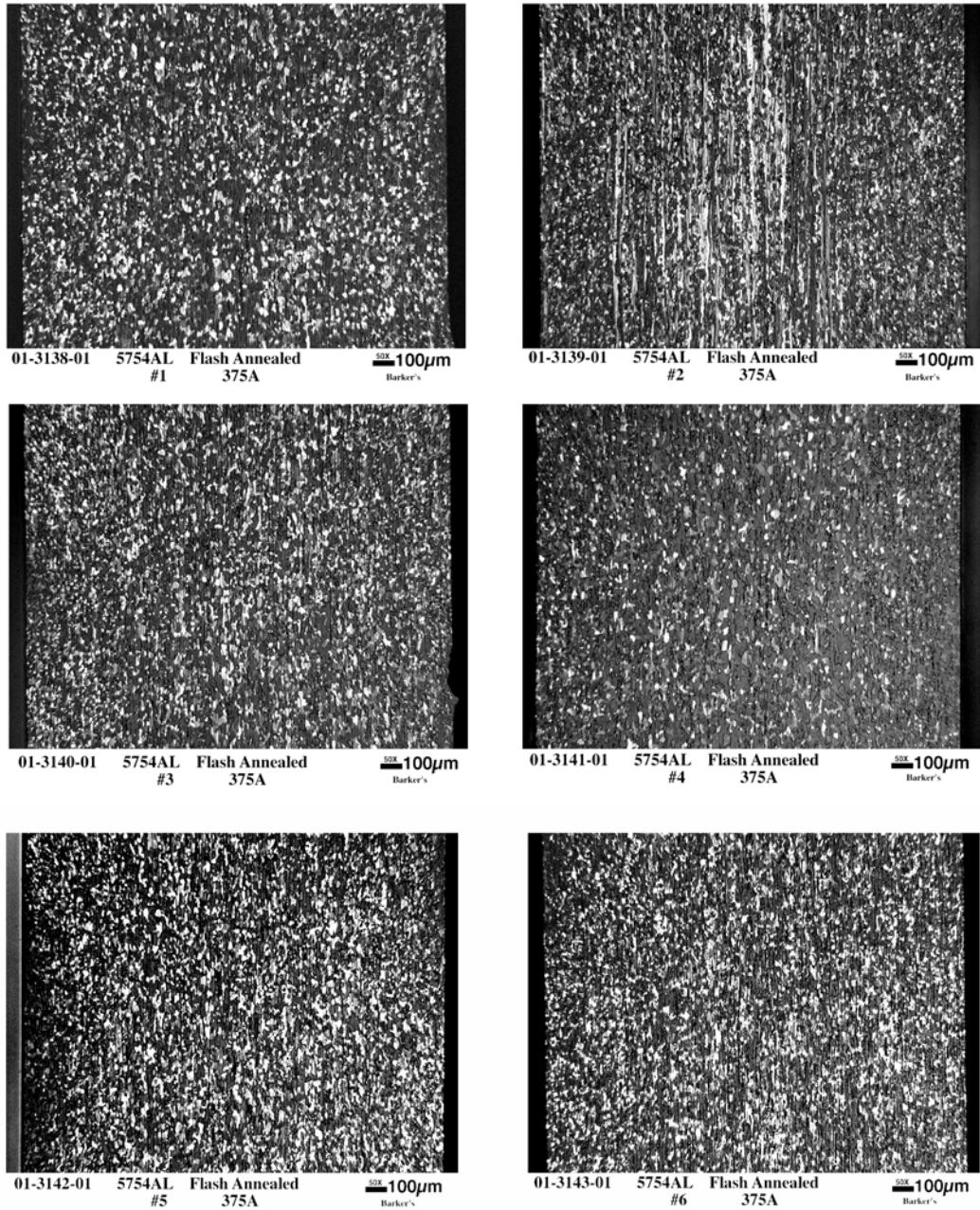


Figure 14. Grain structure of a rolled 5754 Al sample following a plasma arc lamp flash anneal cycle (21°C to 505/540°C in 8 s).

### *Tensile behavior of rapidly annealed samples*

Tensile tests were performed on 5754 aluminum specimens in support of IR plasma annealing studies. All specimen coupons were sectioned from a single 5754 aluminum plate (0.080-in thick) produced at Carson #2 mill. Coupons were IR plasma annealed at 700, 800, and 900°F and a few were resistive heat annealing at 900°F in the Gleeble machine for comparison. After annealing, all the coupons were fabricated in a dog-bone type of tensile specimens having a uniform gage section of 0.25-in wide and 2-in length in conformation to the specimen design recommended by ASTM Standard E8-85a. Tensile tests were performed at room temperature and results are plotted in Figs 15 and 16 for comparison.

Figures 15 and 16 show the tensile behavior in the rolling and transverse orientation, respectively, for the specimens with and without annealing. The yield strength is about 30 ksi and UTS is about 40 ksi in both orientations for specimens in the as-received condition. However, the elongation is about 25% better in the rolling direction. Interestingly, the yield strength fell sharply to about 15 ksi for all of the specimens annealed at 900°F, approximately a half of 30 ksi yield strength for the unannealed. However, the UTS of the annealed fell only by about 25%. The elongation of the annealed specimens increased nominally compared to that of the unannealed by about 10% in the rolling orientation, but doubled in the transverse orientation. The low elongation for the Gleeble annealed specimens is attributed to the localized annealing where only a short section of the gage length was heated to the annealing temperature. In view of the low yield strength and increase in elongation exhibited by the IR plasma annealed specimens, the annealing at 900°F appeared to be effective and the micrographs of post-mortem study support the conclusion. Results of tensile tests on specimens annealed at 800°F or below fell between those of unannealed and fully annealed specimens.

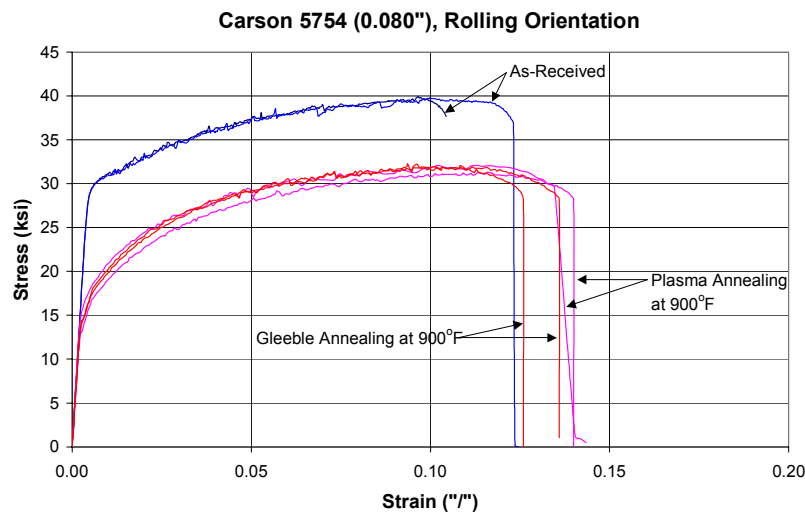


Fig 15 – Comparisons of tensile behavior of 5754 aluminum tested in the as-receive and annealed conditions along the rolling orientation

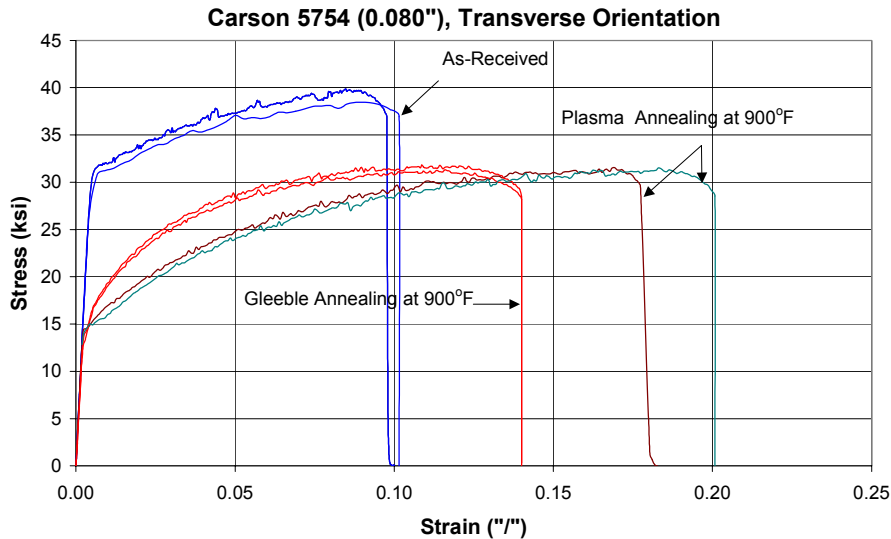


Fig 16 - Comparisons of tensile behavior of 5754 aluminum tested in the as-received, and annealed conditions along the transverse orientation

#### 4.3.4 Modeling of Microstructural Evolution

The objective of this task is to develop a metallurgical model for the in-line recrystallization process, so that the model can be used to develop the optimum in-line processing strategy. In the initial stages of the project, the strategy was to first concentrate on the hot deformation of the hot band itself. One of the consequences of rolling is a deformation gradient in the through-thickness direction of the sheet. It was decided to use a continuum model to determine the thermo-mechanical histories of volume elements at various depths in the sheet, and use the deformation history as input to a microstructural deformation model to determine the deformed microstructure of the hot band as a function sheet depth. These simulated deformation microstructures would then be used in a Monte Carlo based microstructural evolution technique to determine the evolution of microtexture during in-line recrystallization as a function of location in the through-thickness direction. However, during the course of the project, the focus on modeling shifted because of a change in the plant trial schedule, and the need to have a recrystallization kinetics model ready before the plant trials. Therefore, it was decided to develop the input microstructures for recrystallization simulations by characterizing the deformation substructures in the hot band using the EBSP facility at Oak Ridge. The EBSP measurements were to be made at two different locations: the surface and the mid-thickness regions to determine the effect of surface shear on the microtexture after recrystallization.

In this report, the following aspects of modeling that were undertaken in the first year are reported: (1) continuum modeling of hot deformation (2) microstructural evolution modeling of recrystallization and (3) modeling the kinetics of recrystallization

*Continuum Modeling of Hot Deformation:* In this task the hot deformation of AA5754 alloy was modeled using the ABAQUS Explicit finite element code. The thickness of the as-cast material is 0.6” and the it is rolled down to 0.163” in the first pass. In the second-pass the material is rolled from 0.163” to 0.08” thick hot band. The rolls are 8.0” in radius and the linear speed of the as-cast material at the entry of the first roll is 28 ft/ min. The results for the deformation during first pass are reported here. One of the variables in hot rolling is the friction coefficient between the roll and the sheet. The friction coefficient was varied between 0.2 and 0.4 to determine its influence on the through-thickness deformation gradient.

Figure 1 shows the variation in the equivalent plastic strain,  $peeq$ , as a function of depth in the sheet for friction coefficients of 0.2, 0.3 and 0.4. The plastic strain in the surface is seen to increase significantly with increasing friction coefficient. For a friction coefficient of 0.2, there is a small surface layer that has an equivalent plastic strain of 1.6-1.8 while the rest of the thickness has a strain of 1.3 –1.6 as shown in fig. 1a. As the friction coefficient is increased to 0.3, the thickness of the surface layer with strain of 1.3-1.6 increases as shown in fig. 1b. As the friction coefficient increases to 0.4, this layer is seen to increase further. Based on the input from the industrial participants, the friction coefficient in rolling is typically in the range 0.25 to 0.3. The modeling results indicate that under these conditions there should be a significant variation in the through-thickness deformation.

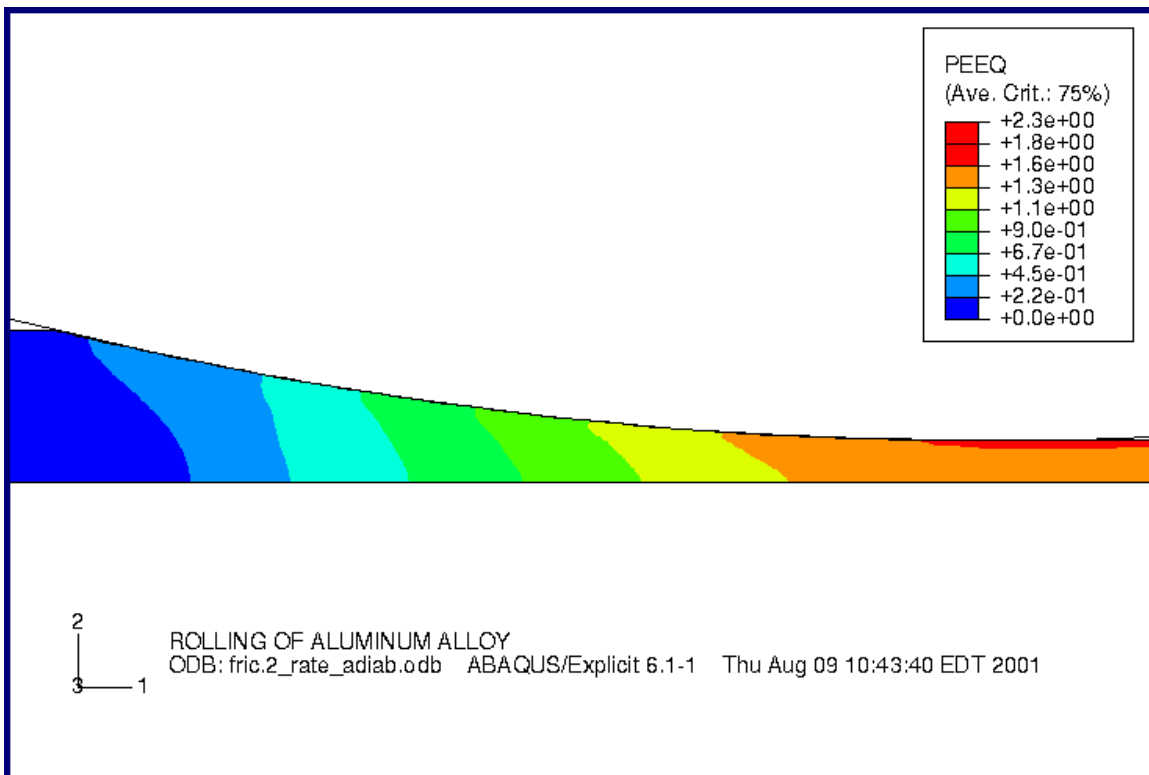


Fig. 1a. Variation of equivalent plastic strain in the through-thickness direction during hot-rolling of AA5754. Friction coefficient between the roll and sheet is 0.2

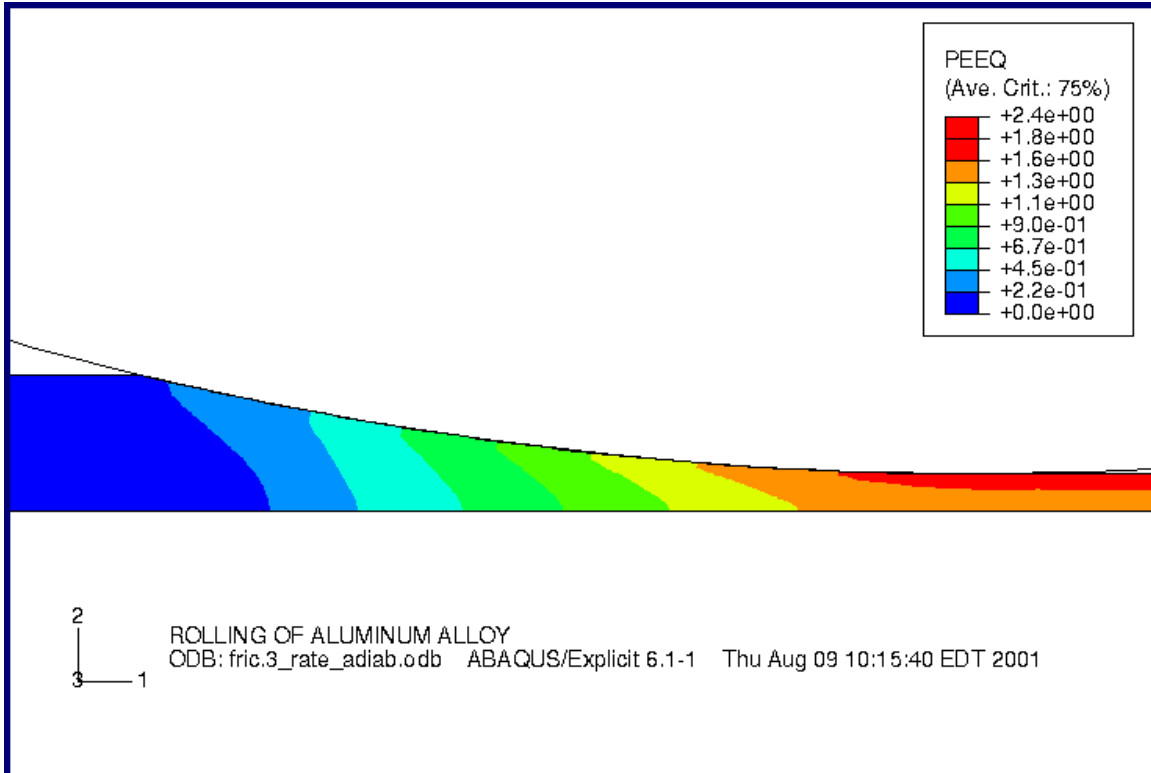


Fig. 1a. Variation of equivalent plastic strain in the through-thickness direction during hot-rolling of AA5754. Friction coefficient between the roll and sheet is 0.3

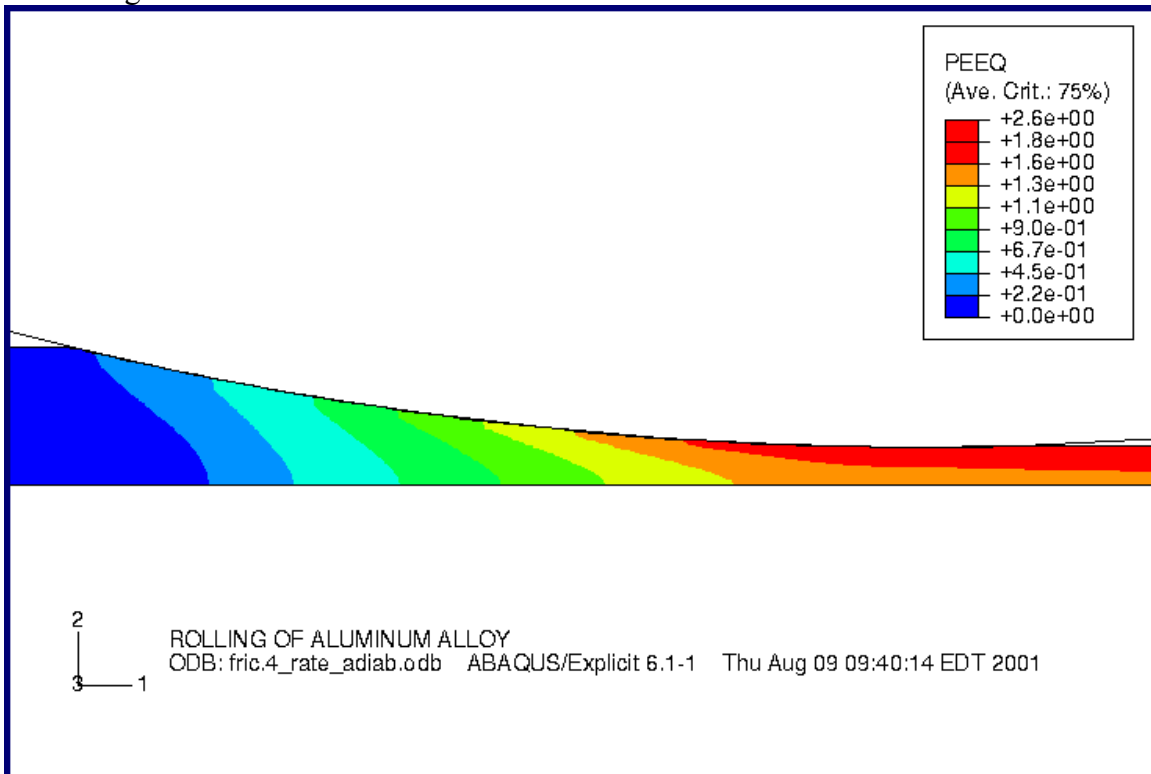
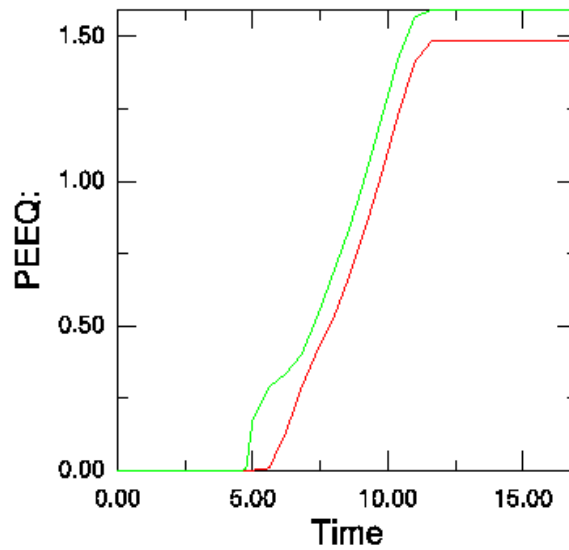
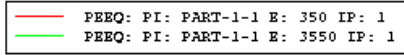
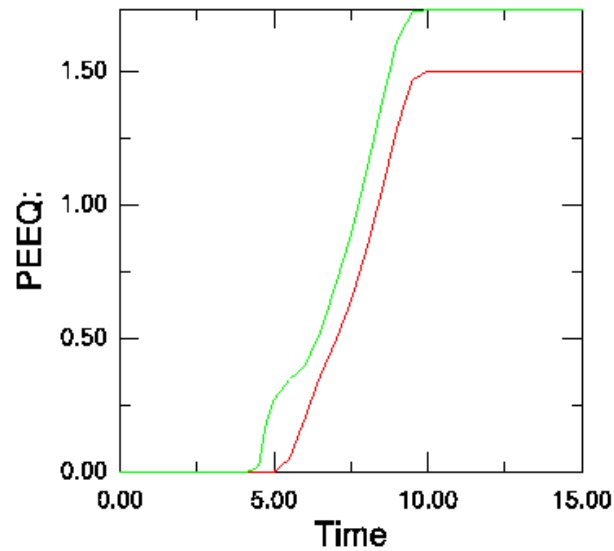
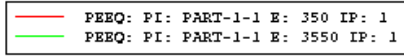


Fig. 1a. Variation of equivalent plastic strain in the through-thickness direction during hot-rolling of AA5754. Friction coefficient between the roll and sheet is 0.4.



(a)



(b)

Figure 2. Variation of equivalent plastic strain for elements on the surface and mid-thickness regions during hot deformation (a) friction coeff. = 0.2 (b) fric. Coeff. = 0.4

Figure 2 shows the variation in the equivalent plastic strain at the surface and mid-thickness region during rolling. It is seen that the difference between the equivalent plastic strains at the surface and mid-thickness increases with friction coefficient. This is

not clearly shown in figure 1 because of the finite number of levels used to represent the plastic strain contours.

There is a qualitative agreement between the model predictions and experimental data with regard to the variation of stored energy of deformation in the through-thickness direction. A higher plastic strain (and therefore, a higher stored energy of deformation) in the surface compared to the center will result in faster recrystallization kinetics at the surface, and also will result in a finer recrystallized grain size. This trend can be seen very clearly in the micrographs shown in figure 14, section 4.3.3.2, for samples recrystallized by rapid heating using infrared.

*Modeling of microstructural evolution during recrystallization:* As described previously, the deformation modeling effort was discontinued because of time constraints, and it was decided to focus on the recrystallization modeling effort, using input microstructural data obtained by EBSD analysis. Accordingly, the existing MC microstructural simulation code was adapted to handle input data from EBSD measurements.

The input microstructure used in the simulations corresponds to figure A in section 4.3.1. The material is AA5754, 0.08" hot band, and the EBSD scan was obtained from the RD-TD plane and a section close to the top surface. The total scan area is  $160 \times 210 \mu\text{m}^2$  and the step size of the scan is  $0.6 \mu\text{m}$ . The input data consisting of the coordinates of the scan sites and the Euler angles corresponding to each location were mapped on to a two-dimensional triangular lattice. The subgrain growth was simulated using a Monte Carlo simulation where the local energy calculations were performed using the first-nearest neighbor consisting of six sites. The relative boundary energy as a function of boundary misorientation was calculated using the Read-Schockley model, and the relative boundary mobility as a function of misorientation was calculated according to a sigmoidal relationship. The details of the simulation are included in this report. For those boundaries whose misorientation corresponds to a rotation about a  $\langle 111 \rangle$  type axis, the boundary energy and mobility were obtained from previously determined molecular dynamics simulation data. The time evolution of the microstructure due to recrystallization is shown in figure 3.

The initial hot band microstructure consists of a large number of small cells approximately 2-3 microns in diameter. Recrystallization involves the abnormal growth of these subgrains to form large grains. In the microstructures shown in figure 3, the green lines correspond to high angle boundaries with misorientations greater than  $15^\circ$ . It is seen that these boundaries are clustered in certain areas of the microstructures. It appears that these boundaries are present in the vicinity of second phase particles. However, during the recrystallization simulation, these boundaries disappeared quickly, although these sites appear to be the origin of the abnormally growing grains. Figure 4 shows the initial texture of the hot band and the simulated texture after recrystallization in the form of  $\langle 100 \rangle$  contour plots. Recrystallization appears to strengthen the S deformation texture component and reduce the Brass component. However, there is no indication of the formation of cube texture, which is normally found during recrystallization following hot deformation of DC materials.

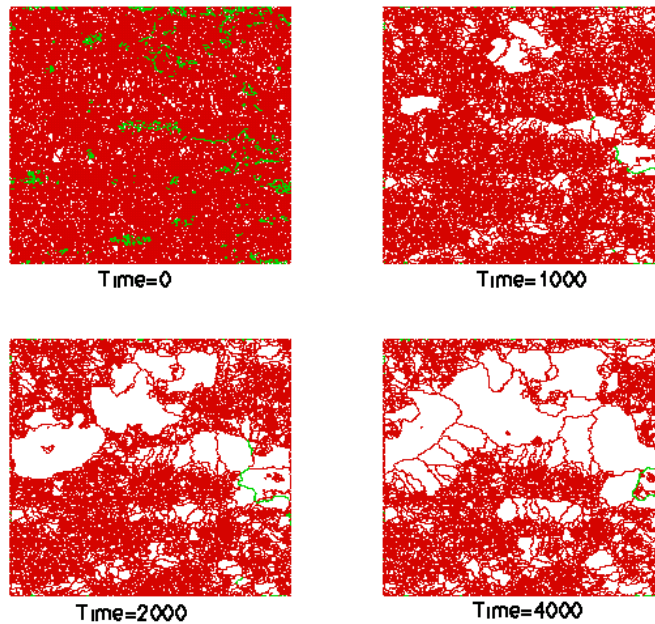


Figure 3. Simulation of microstructural evolution during recrystallization of AA5754 hot band.

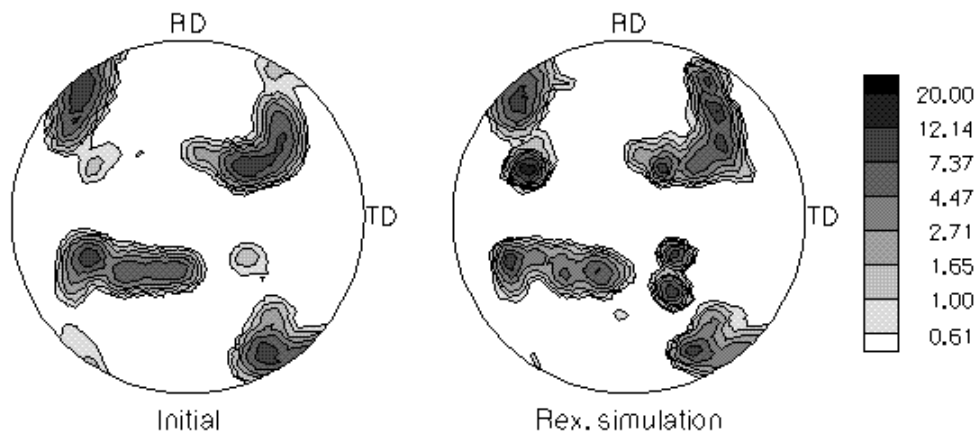


Figure 4.  $\langle 100 \rangle$  contour plots of 5754 hot band RD-TD surface plane and the simulated recrystallization texture

The mechanism by which cube texture forms during recrystallization is well documented in the literature for DC materials. In these materials, the cube components are initially present prior to hot deformation, they survive the hot deformation process, and are present in the hot band as sheets. These persistent cube bands are known to be the nuclei for the cube component during recrystallization. The reason that cube component does not evolve in the CC material is because of the absence of such cube bands.

Figure 5 shows the hot band microstructure, and the regions that are in the vicinity of the cube orientation. Notice that the initial cube orientations are few and small in size. It is

possible that the cells that are in the cube orientation are large enough to possess the required size advantage for initiating abnormal growth.

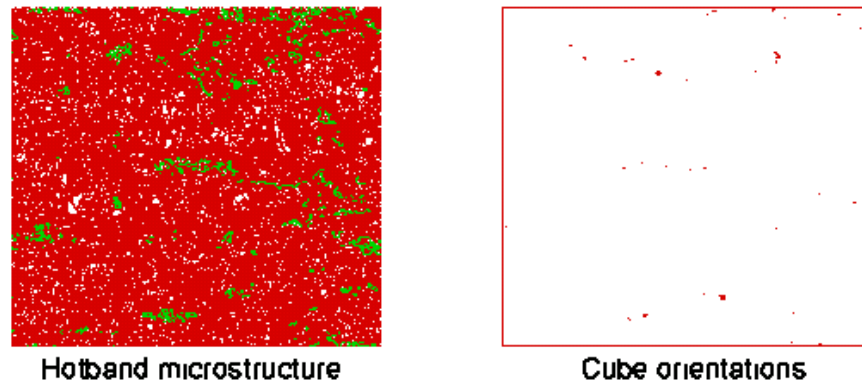


Figure 5. The distribution of near-cube orientations in the hot band microstructure of AA5754, RD-TD surface plane.

The EBSD data shown in section 4.3.1 (figures B and D) indicates that the texture in the RD-TD surface plane as well as in the mid-thickness plane becomes more random as a result of recrystallization. The strong deformation texture is significantly reduced. Such a phenomenon has not been reported in the recrystallization of DC alloys. It is not clear whether the phenomenon is due to the inherent differences between the CC and DC materials, or it is due to the rapid heating process. Clearly, the simulations do not capture the randomization of the recrystallization texture.

*Modeling of Recrystallization Kinetics:* The objective of this modeling effort is to calculate the apparent activation energy for recrystallization, which is required for calculating the recrystallization kinetics under continuous heating conditions. The approach is to obtain the recrystallization curves at 3 or 4 different temperatures that are in the range of temperatures that the hot band goes through during in-line annealing. Temperatures of 800F, 830F and 860F were used for this purpose. The samples were annealed as described in section 4.3.3.2. The yield strength after the various isothermal holds was determined, and the results are shown in figure 6a. It is assumed that the percentage change in yield strength due to recrystallization is proportional to the volume fraction of recrystallization at these temperatures. The percent recrystallized as a function of isothermal hold time is shown in figure 6b. Additional data for annealing at 880F are being obtained. These data will also be used in the calculation of activation energy. The apparent activation energy for recrystallization is obtained by plotting the logarithm of time for 50% recrystallization,  $t_{0.5}$ , versus  $1/T$  where  $T$  is the recrystallization temperature in Kelvin. Based on the available data at 800F, 830F and 860F, the Arrhenius plot of  $\ln t_{0.5}$  versus  $1/T$  is shown in figure 7. From the slope of the straight line, an activation energy of 16,350 cal/mole has been obtained. This number will be further refined when more isothermal recrystallization data become available in the future.

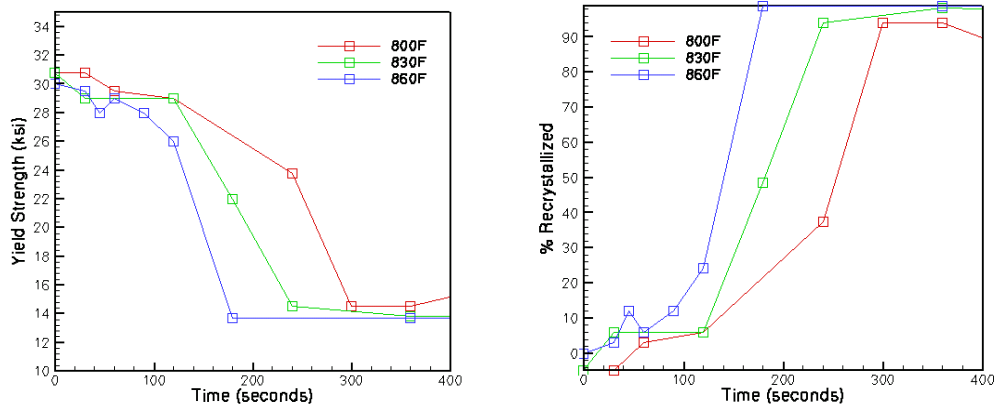


Figure 6. Isothermal recrystallization data showing the yield strength (left) and the percent recrystallized (right) as a function of recrystallization time.

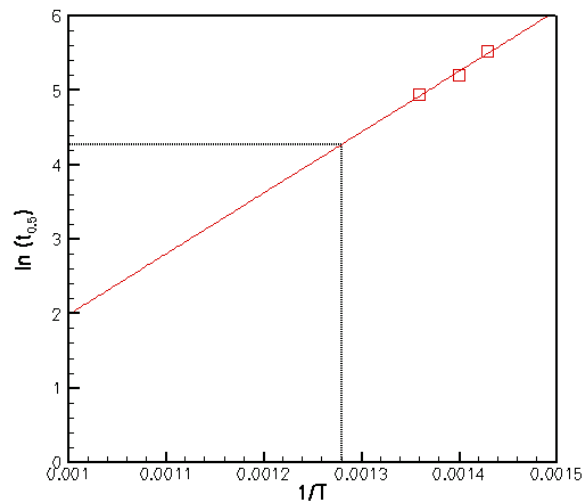


Figure 7. Plot of  $\ln(t_{0.5})$  versus  $1/T$  to calculate the apparent activation energy for recrystallization.

From figure 7, it is possible to calculate the time for 50% recrystallization at 950F. The data for 950F is shown by the dotted lines in figure 7. The time for 50% recrystallization at 950F is calculated as 74 seconds. However, the IR heating experiments clearly indicate that the recrystallization at 950F is almost complete in 1 s at 950F. Therefore, there seems to be a discrepancy between the 950F experimental kinetics data and the kinetics obtained by extrapolating the data in figure 7. Such a discrepancy is possible if the activation energy for the process changes or if there is a change in the mechanism of recrystallization. Microstructural changes such precipitation and dissolution of second phase(s) can significantly alter the recrystallization kinetics.

Preliminary calculations of thermodynamic equilibrium of phases in 5754 was carried out using Thermocalc. The nominal composition of 5754 was in these calculations was Al-0.095Si-0.239Fe-0.028Cu-0.316Mn-2.854Mg-0.011Cr-0.001Zr. The thermodynamic calculations indicated that the Al<sub>6</sub>Mn precipitate is stable in this alloy system in the temperature range where isothermal recrystallization experiments were carried out. The dissolution temperature of Al<sub>6</sub>Mn is calculated to be 860F. Therefore, it is possible that the dissolution of Al<sub>6</sub>Mn results in a drastic increase in the recrystallization kinetics at temperatures above 860F since the subgrains in the hot worked microstructure would no longer be pinned by the precipitates at these temperatures. Further characterization of samples recrystallized at these temperatures should be carried out in order to verify this hypothesis.

#### 4.4 In-plant Trials (Ajax Magnethermic and Commonwealth)

The objective of this task is to design, fabricate and install an in-line annealing system based on induction heating at the Carson, California plant, and conduct in-line annealing experiments. Drawings and design details of the proposed in-line annealing unit were discussed at the project review meeting held on August 24<sup>th</sup>, 2001. The designed unit is expected to be 72" long to keep the current density at a reasonable level and will have capacitor banks on both sides, which is not a very common feature. Conveyor belts are used to guide the strip into the narrow gap between the coils. Design and fabrication of the heating unit has been completed and the unit has been installed at the Carson plant. The plant trials are expected to take place in March 2002.

#### 5.0 Summary

All the tasks that were envisioned for the project are well under way and the progress is quite satisfactory. The IR heating technique to generate samples for formability testing has been standardized and is set for supplying the required samples to Univ. of Michigan and Univ. of Kentucky. Advanced characterization using EBSD posed initial challenges with regard to sample preparation technique, but these challenges have been overcome. There is a problem with the data acquisition system that limits the size of the data files used in microstructural modeling. The solution to this problem has already been identified and is being addressed. The microstructural modeling task is proceeding satisfactorily. It appears that precipitation and dissolution of Mn-rich precipitates could play a significant role in the kinetics of recrystallization during in-line annealing. This aspect will be further investigated in the second year of the project. Texture predictions will require the use of larger input files using high-resolution EBSD data. With the introduction of a proposed new PC based data acquisition system, it should be possible to generate such data from EBSD and used as input to microstructural modeling. The characterization of mechanical properties of cold worked and annealed hot band at University of Kentucky and University of Michigan is on schedule, and formability testing using rapidly annealed laboratory samples will be carried out next year.